NAVAL POSTGRADUATE SCHOOL

MONTEREY, CALIFORNIA

THESIS

PEAK POWER CONTROL WITH AN ENERGY MANAGEMENT SYSTEM

by

Nathan J. Peck

March 2013

Thesis Co-Advisors: Giovanna Oriti
Alexander L. Julian

Approved for public release; distribution is unlimited

THIS PAGE INTENTIONALLY LEFT BLANK

REPORT DOCUMENTATION PAGE			Form Approved OMB No. 0704–0188
Public reporting burden for this collection of information is estimated to average 1 hour per response, including the time for reviewing instruction, searching existing data sources, gathering and maintaining the data needed, and completing and reviewing the collection of information. Send comments regarding this burden estimate or any other aspect of this collection of information, including suggestions for reducing this burden, to Washington headquarters Services, Directorate for Information Operations and Reports, 1215 Jefferson Davis Highway, Suite 1204, Arlington, VA 22202–4302, and to the Office of Management and Budget, Paperwork Reduction Project (0704–0188) Washington DC 20503.			
1. AGENCY USE ONLY ***(Leave blank)***	**2. REPORT DATE** March 2013	**3. REPORT TYPE AND DATES COVERED** Master's Thesis	
4. TITLE AND SUBTITLE PEAK POWER CONTROL WITH AN ENERGY MANAGEMENT SYSTEM			**5. FUNDING NUMBERS** N/A
6. AUTHOR(S) Nathan J. Peck			
7. PERFORMING ORGANIZATION NAME(S) AND ADDRESS(ES) Naval Postgraduate School Monterey, CA 93943–5000			**8. PERFORMING ORGANIZATION REPORT NUMBER**
9. SPONSORING /MONITORING AGENCY NAME(S) AND ADDRESS(ES) N/A			**10. SPONSORING/MONITORING AGENCY REPORT NUMBER**
11. SUPPLEMENTARY NOTES The views expressed in this thesis are those of the author and do not reflect the official policy or position of the Department of Defense or the U.S. Government. IRB Protocol number _____N/A_____.			
12a. DISTRIBUTION / AVAILABILITY STATEMENT Approved for public release; distribution is unlimited			**12b. DISTRIBUTION CODE**

13. ABSTRACT (maximum 200 words)

The Department of Defense (DoD) is researching methods to enhance energy security and reduce energy costs. The energy security of DoD installations relies on the commercial electricity grid. One method being considered to improve energy security and reduce energy costs is microgrids that include combinations of energy storage, energy sources, critical loads, and non-critical loads. A microgrid's power demand and the benefits of a microgrid integrated with a power electronics enabled Energy Management System (EMS) is investigated in this thesis. The power demand of a single family household is analyzed. The peak power demand of the single family household displays the drawbacks of peak power demand on the commercial electricity grid and the installations receiving power from it. Drawbacks include reduced energy security due to blackouts and increased cost as a result of meeting the peak demand. One benefit of an EMS is its ability to island or continue supplying power to critical loads when the commercial electricity grid is lost. A second benefit is reduced power demand on the commercial electricity grid during peak power demand or on distributed resources (DR) while islanded by performing peak power control. The performance of peak power control by an EMS is demonstrated using a Simulink model and an experimental laboratory setup. The Simulink model and EMS functionality are validated with the laboratory experiments. The Simulink model is then used to demonstrate the reduction in peak power demand on the commercial electricity grid using an EMS on more complex loads such as motors and diode rectifiers. The Simulink model is also used to compare the power demand on the commercial electricity grid with and without the EMS.

14. SUBJECT TERMS Energy Management System, Microgrid			**15. NUMBER OF PAGES** 91
			16. PRICE CODE
17. SECURITY CLASSIFICATION OF REPORT Unclassified	**18. SECURITY CLASSIFICATION OF THIS PAGE** Unclassified	**19. SECURITY CLASSIFICATION OF ABSTRACT** Unclassified	**20. LIMITATION OF ABSTRACT** UU

THIS PAGE INTENTIONALLY LEFT BLANK

Approved for public release; distribution is unlimited

PEAK POWER CONTROL WITH AN ENERGY MANAGEMENT SYSTEM

Nathan J. Peck
Lieutenant, United States Navy
B.S., United States Naval Academy, 2005

Submitted in partial fulfillment of the
requirements for the degree of

MASTER OF SCIENCE IN ELECTRICAL ENGINEERING

from the

NAVAL POSTGRADUATE SCHOOL
March 2013

Author: Nathan J. Peck

Approved by: Giovanna Oriti
Thesis Co-Advisor

Alexander L. Julian
Thesis Co-Advisor

R. Clark Robertson
Chair, Department of Electrical and Computer Engineering

THIS PAGE INTENTIONALLY LEFT BLANK

ABSTRACT

The Department of Defense (DoD) is researching methods to enhance energy security and reduce energy costs. The energy security of DoD installations relies on the commercial electricity grid. One method being considered to improve energy security and reduce energy costs is microgrids that include combinations of energy storage, energy sources, critical loads, and non-critical loads. A microgrid's power demand and the benefits of a microgrid integrated with a power electronics enabled Energy Management System (EMS) is investigated in this thesis. The power demand of a single family household is analyzed. The peak power demand of the single family household displays the drawbacks of peak power demand on the commercial electricity grid and the installations receiving power from it. Drawbacks include reduced energy security due to blackouts and increased cost as a result of meeting the peak demand. One benefit of an EMS is its ability to island or continue supplying power to critical loads when the commercial electricity grid is lost. A second benefit is reduced power demand on the commercial electricity grid during peak power demand or on distributed resources (DR) while islanded by performing peak power control. The performance of peak power control by an EMS is demonstrated using a Simulink model and an experimental laboratory setup. The Simulink model and EMS functionality are validated with the laboratory experiments. The Simulink model is then used to demonstrate the reduction in peak power demand on the commercial electricity grid using an EMS on more complex loads such as motors and diode rectifiers. The Simulink model is also used to compare the power demand on the commercial electricity grid with and without the EMS.

THIS PAGE INTENTIONALLY LEFT BLANK

TABLE OF CONTENTS

LIST OF FIGURES

LIST OF ACRONYMS AND ABBREVIATIONS

A/D	Analog/Digital
DC	Direct Current
DER	Distributed Energy Resources
DG	Distributed Generators
DoD	Department of Defense
DR	Distributed Resources
EMS	Energy Management System
FPGA	Field Programmable Gate Array
IGBT	Insulated Gate Bipolar Transistor
I/O	Input/Output
ISE	Integrated Software Environment
IPM	Integrated Power Module
JTAG	Joint Test Action Group
PC	Personal Computer
PCB	Printed Circuit Board
PI	Proportional-Integral Controller
PSC	Permanent Split Capacitor
PV	Photovoltaic
PWM	Pulse Width Modulation
SCR	Silicon Controller Rectifier
SDC	Student Design Center
TTL	Transistor Transistor Logic
USB	Universal Serial Bus
VHDL	VHSIC Hardware Description Language
VHSIC	Very High Speed Integrated Circuits

THIS PAGE INTENTIONALLY LEFT BLANK

EXECUTIVE SUMMARY

The Department of Defense (DoD) is researching methods to enhance energy security and reduce energy costs [1]. One method the DoD is researching to increase energy security and reduce energy cost is making DoD facilities into self-sustainable systems or microgrids. A microgrid is a combination of energy storage, energy sources, critical loads and non-critical loads [2], [3]. A microgrid controlled by a power electronics based energy management system (EMS) can optimize the use of energy sources and energy storage systems to provide improved energy security and reduced energy cost. Specifically, an EMS can reduce a microgrid's peak power demand on the commercial electricity grid or on distributed resources (DR). A block diagram of an EMS interfaced with the commercial electricity grid and a microgrid is shown in Figure 1.

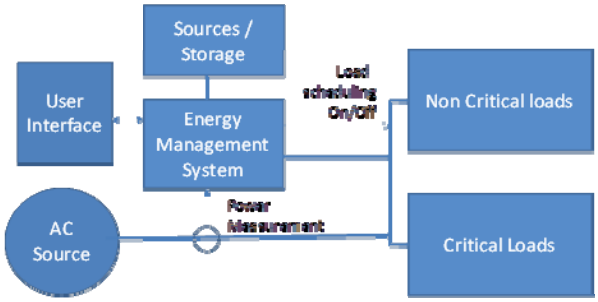

Figure 1. An EMS interfaced with the commercial electricity grid and a microgrid.

The objective of this thesis was to investigate peak power demand of a microgrid and to perform peak power control using a power electronics based EMS that reduces a microgrid's peak power demand such that energy security is improved and energy cost reduced. A physics based model was developed and validated using experimental prototyping, and then the model was used to simulate peak power control.

An EMS creates the opportunity to manipulate power intelligently in a microgrid. Its functionality is demonstrated by modeling, simulation and experimental validation of the following scenarios:

1) Peak power control by tapping an energy storage system during high demand.

2) Islanding mode by necessity (loss of power) or by choice.

3) Peak power control by non-critical load shedding during transients.

By accomplishing these goals, the EMS can be very useful in commercial electricity grid connected systems where there is a limit on the user's power consumption. If the EMS keeps the load current below a set threshold at all times by load management and shedding, then the user can operate loads beyond their steady-state power limits without worrying about the circuit breaker interrupting power.

Three scenarios are illustrated in Figure 2, where a microgrid with a single-phase power source and a battery pack is used to demonstrate the functionality of the EMS. The first scenario demonstrates how the peak rms current drawn from the main power source is limited by the EMS when the critical load increases. The EMS behaves as a current source, providing the supplemental current demanded by the loads and reducing the current demand on the main power source. The second scenario demonstrates islanding mode of operation. Islanding of the microgrid can occur when the load is so light that the battery, or stored energy, can provide all its current or when there is a fault or poor power quality in the main power source. In the second scenario, the EMS inverter operates as a voltage source. The third scenario demonstrates how the EMS can shed a non-critical load when the critical load increases, thus keeping the source rms current below a set threshold. The third scenario first provides supplemental current to reduce the main power source rms current and then sheds non-critical loads to maintain the main power source rms current below the set threshold.

The EMS control algorithm was developed with the following goals, listed here in order of priority:

1) Power must be available to the critical loads at all times. As an example, if the main power supply (commercial electricity grid) is down, then battery power will be used to support critical load operation.

2) Reduce the peak power demand of the microgrid on the main power source by using battery power and by non-critical load shedding.

3) Maximize the state of charge of the battery.

4) Make power available to non-critical loads.

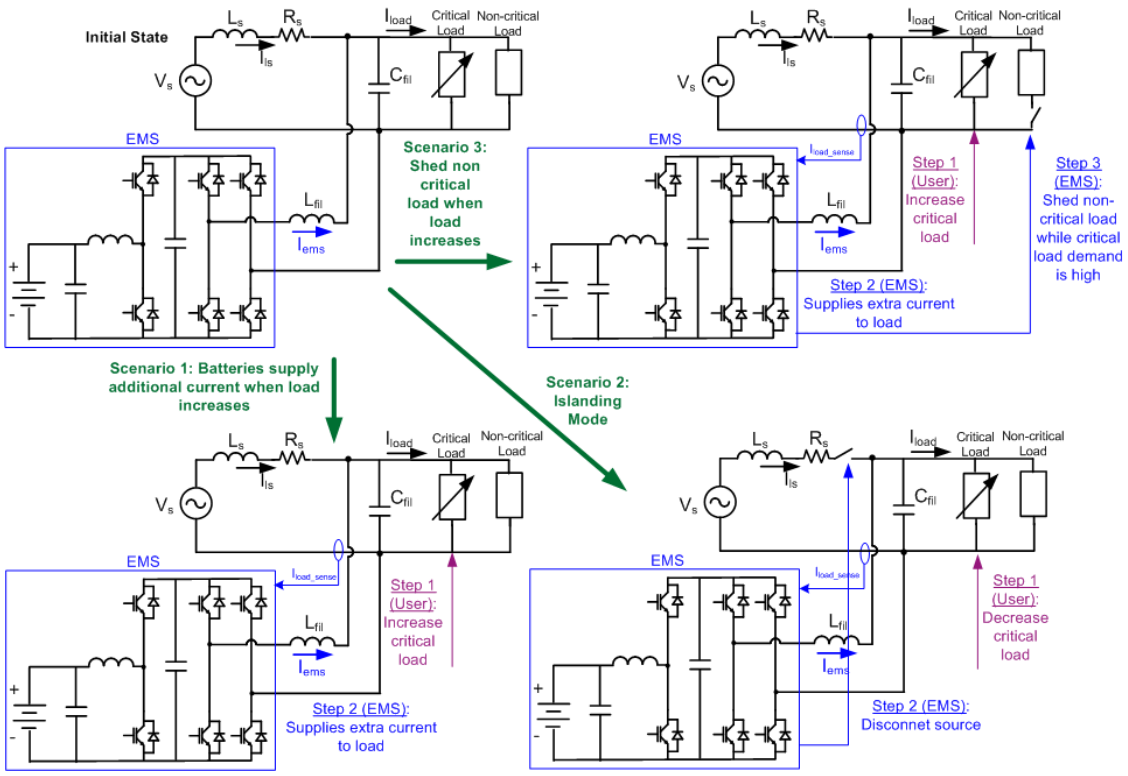

Figure 2. The scenarios used to demonstrate EMS functionality.

A physics based model of the EMS was developed and implemented using Simulink software [4]. The model was validated using a power electronics based power conversion system designed to support laboratory development and rapid experimental validation for research and thesis projects [5] – [8]. The system includes a field programmable gate array (FPGA) development board [9] with input/output (I/O) ports, an insulated gate bipolar transistor (IGBT) power module, power supply, voltage/current sensors, analog/digital (A/D) converters, transistor-transistor logic (TTL) interface and a USB interface to communicate with a personal computer (PC).

The microgrid model, validated by experimental measurements, was used to simulate the EMS functionality in a microgrid. The circuit for the simulation has two critical loads and two non-critical loads. The two critical loads are a single-phase diode rectifier and a resistor. The two non-critical loads are a capacitor-start, capacitor-run single-phase induction machine and a resistor. The EMS prioritized the non-critical machine load above the non-critical resistive load.

Simulation results are shown in Figure 3, Figure 4, and Figure 5 for the following modes of operation, respectively:

i. The EMS is fully operational. The EMS provides half of the load current I_{load} when the load current I_{load} is larger than the EMS current threshold $I_{ems\text{-}on}$. A non-critical load is shed when the load current I_{load} exceeds the load shedding threshold I_{max}.

ii. The EMS is operational without load shedding enabled. The EMS provides half of the load current I_{load} when the load current I_{load} is larger than the EMS current threshold $I_{ems\text{-}on}$ but does not control the non-critical loads.

iii. The EMS is disabled.

In the simulation plots of Figure 3, the following events are labeled:

1) The EMS current I_{ems} turns on because the load current I_{load} crosses the EMS current threshold $I_{ems\text{-}on}$.

2) The non-critical resistive load is shed because the load current I_{load} exceeds the load shedding threshold I_{max}.

3) The single-phase induction machine transitions from capacitor start to capacitor run, which reduces the load current I_{load} but has no effect on EMS operation.

4) The diode rectifier is turned off and the load current I_{load} goes below the shed load restoration threshold I_{maxoff}.

5) The non-critical resistive load previously shed is now turned back on automatically.

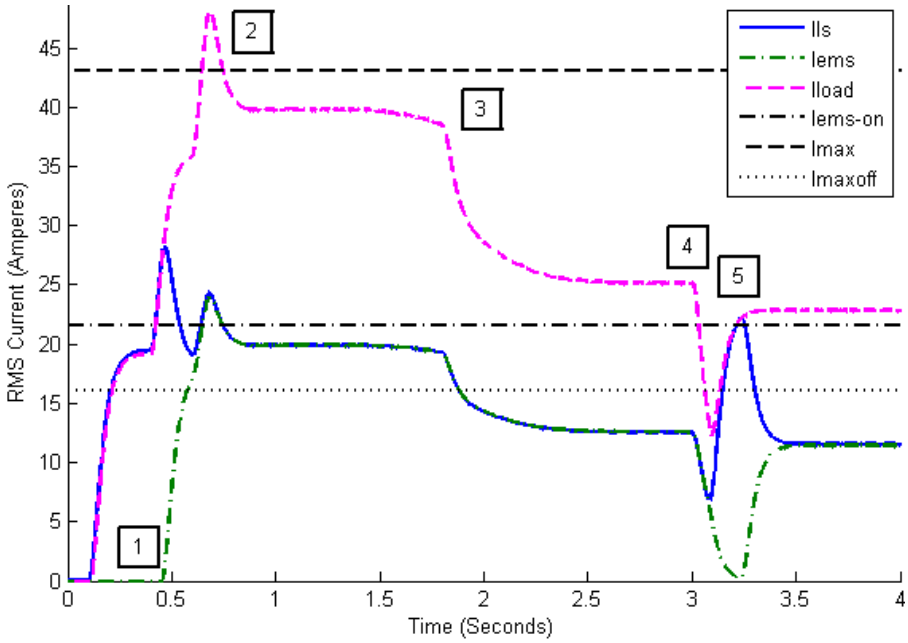

Figure 3. Simulation plots with the EMS fully operational.

The EMS was fully operational for the simulation illustrated in Figure 3. It can be seen in Figure 3 that when the load current I_{load} exceeds the EMS current threshold $I_{ems\text{-}on}$, the EMS supplies current to reduce the main power source current I_{ls}. When the load current I_{load} exceeds the load shedding threshold I_{max}, the non-critical resistive load is shed to reduce the main power source current I_{ls}. Lastly, when the load current I_{load} drops below the shed load restoration threshold I_{maxoff}, the non-critical resistive load is restored.

The advantage of operating with load shedding enabled is that the load current I_{load} only briefly exceeds the maximum current threshold I_{max} established before shedding non-critical loads. The disadvantage is that the non-critical load may not be restored automatically when the system can support restoration of it. This can be seen in Figure 3 after the machine load transitions to its capacitor-run circuitry, the non-critical resistive

load is not restored even though the system can support it. This is due to the limited capability of the EMS algorithm at this time and may be overcome by more capable algorithms in the future.

In the simulation plots of Figure 4, the following events are labeled:

1) The EMS current I_{ems} turns on because the load current I_{load} crosses the EMS current threshold $I_{ems\text{-}on}$.

2) The single-phase induction machine turns on, but no loads are shed and the load current I_{load} exceeds the load shedding threshold I_{max}.

3) The single-phase induction machine transition from capacitor start to capacitor run occurs and causes the load current I_{load} to drop below the load shedding threshold I_{max}.

4) The diode rectifier is turned off but does not affect EMS operation.

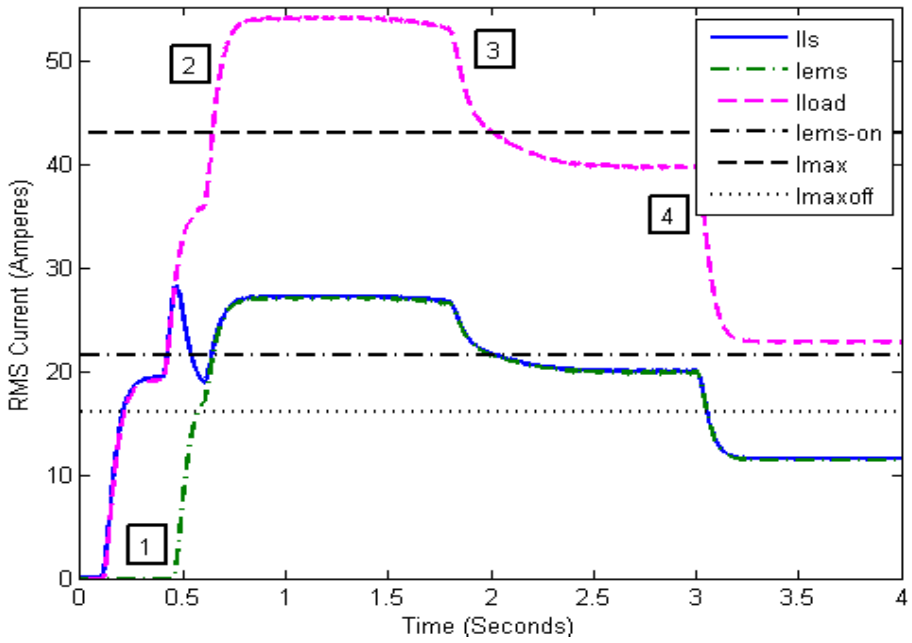

Figure 4. Simulation plots with the EMS load shedding disabled.

The mode of operation with the EMS enabled but without the load shedding capability is illustrated in Figure 4. The disadvantage of operating without load shedding

is that the system may exceed the maximum load current threshold I_{max}, which could result in loss of power to the entire system instead of just the non-critical loads. Comparing Figure 3 and Figure 4, we see that the load current peak is measurably reduced by the load shedding feature of the EMS. As a consequence, the peak of the current drawn from the main power source I_{ls} is reduced.

Without the EMS operating, the disadvantage is a less efficient and more robust main power source that must be capable of handling the peak power demand of its loads as shown in Figure 5.

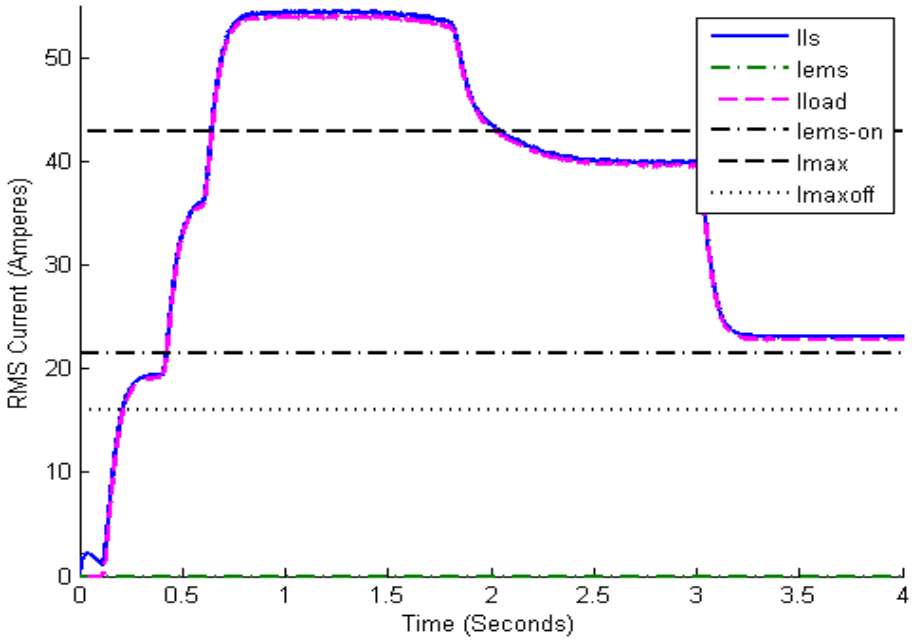

Figure 5. Simulation plots with the EMS disabled.

This research presented problems associated with DoD facilities related to energy security and cost. It focused on the incorporation of electrical microgrids and DR within the present electrical distribution of DoD facilities as a solution. The functionality of a power electronics based EMS was discussed. A physics based model was experimentally validated and then used to compare the operation of a microgrid with and without the EMS.

LIST OF REFERENCES

[1] J. Marqusee. (2012, March 8). Innovation and installation energy. [Online]. Available: http://www.nps.edu/video/portal/Video.aspx?enc=Rp05qxtdJ8MtSo72lcJ4T9895F6NfRNu.

[2] R.H. Lasseter, "MicroGrids" in *Proc. of IEEE Power Engineering Society Winter Meeting,* New York, NY, pp. 305–308, January 2002.

[3] R. H. Lasseter, "Smart distribution: Coupled microgrids," in *Proc. of the IEEE* vol. 99, no. 6, pp. 1074–1082, June 2011.

[4] Simulink® by MathWorks [Online] http://www.mathworks.com/products/simulink/

[5] J. E. O'Connor, "Field programmable gate array control of power systems in graduate student laboratories," M.S. thesis, Naval Postgraduate School, Monterey, CA, March 2008.

[6] G. Oriti, D. Zulaica, A.L. Julian, and R. Cristi, "Hardware laboratories for power electronics and motor drives distance learning courses" in *Proc. of IEEE 2nd Energy Conversion Conference and Expo (ECCE) 2010*, Atlanta, GA, Sept 2010.

[7] G. Oriti and A.L. Julian, "Three phase VSI with FPGA based multisampled space vector modulation," *IEEE Trans. on Industry Applications*, vol. 47, no.4, Jul/Aug 2011.

[8] G. Oriti, A.L. Julian, and D. Zulaica, "Doubly fed induction machine drive distance learning laboratory for wind power and electric ship propulsion applications," in *Proc. of IEEE 3rd Energy Conversion Conference and Expo (ECCE)* 2011, Phoenix, AZ, Sep 2011.

[9] Xilinx® "Avnet Virtex-4 LC Development Board," online at: http://www.xilinx.com/products/devkits/DS-KIT-4VLX25LC.htm.

ACKNOWLEDGMENTS

I would like to thank my amazing wife, Julia, and my darling baby girl, Clara, for their support and patience while I was absorbed in my research. Your love and care mean everything to me. I love you both with all my heart.

I would like to thank Dr. Giovanna Oriti and Dr. Alexander Julian for their amazing tutelage in and outside the classroom. I learned a great deal more about this subject matter and many other subjects than this thesis addresses. Both of you were patient and always available to direct or redirect my research, while also kindly reminding me of the ultimate goal, to learn something.

I would like to thank CDR Brian Davies for supporting my attendance of the Naval Postgraduate School and for his continued support in all my endeavors' in the U.S. Navy. Your example on the boat and off the boat has left a lasting impression.

Lastly, I would like to thank my parents, Steven and Janet Peck, for supporting me for so long and always being there with advice and a gentle nudge in the right direction. I love you both.

THIS PAGE INTENTIONALLY LEFT BLANK

I. INTRODUCTION

A. BACKGROUND

The Department of Defense (DoD) is researching methods to enhance energy security and reduce energy costs [1]. The energy security of DoD facilities rely on the commercial electricity grid. This places the operations of these facilities and the missions they support at risk. Additionally, the DoD energy costs, illustrated in Figure 1 for fiscal year 2011, due to facilities electrical demand was 65% of $4.12 billion, or $2.7 billion dollars. This makes up 13.65% of all DoD energy costs [1].

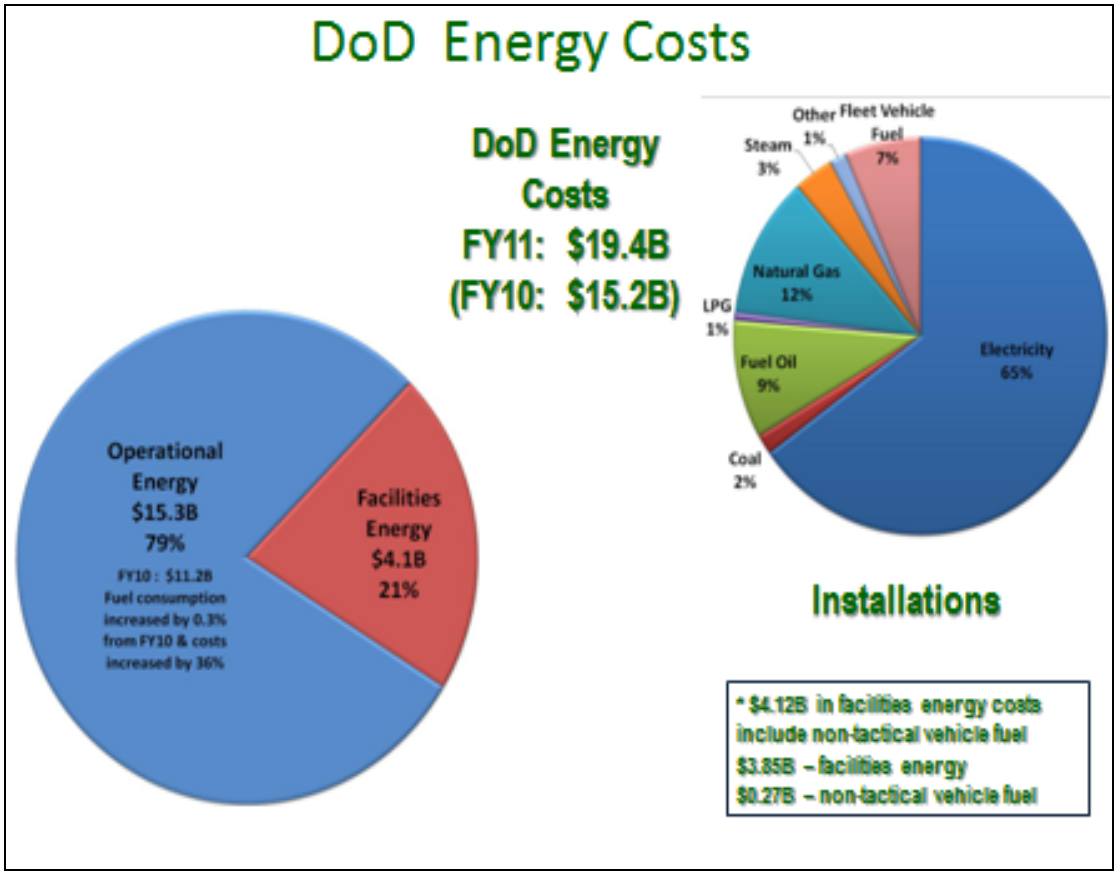

Figure 1. DoD energy costs. From [1].

One method the DoD is researching to increase energy security and reduce energy cost is making DoD facilities into self-sustainable systems or microgrids. A microgrid is

a combination of energy storage, energy sources, critical loads and non-critical loads [2], [3]. Energy storage and energy sources consist of distributed resources (DR) and/or the main power grid. DR or distributed energy resources (DER) are sources of electric power that are not directly connected with a bulk power transmission system [4]. They include energy generation and storage such as internal combustion engines, gas turbines, microturbines, photovoltaic (PV) systems, fuel cells, batteries and wind-power [3], [5]. Critical loads must be serviced at all times, while non-critical loads can be shed if power is insufficient. Thus, a microgrid is an integrated energy system that can operate in parallel with the grid or as an island. Objectives related to improved reliability, enhanced electrical system security, increased integration of renewable resources, and dynamic islanding can be realized through the use of microgrids [3], [5].

Power electronics is a key enabling technology to interface DR to the grid and to provide the control features necessary to build a more controllable power system [6]–[8]. A digitally controlled power electronics based energy management system (EMS) can provide power flow metering and control, fault detection and correction, reliability improvements, improved electrical system security, increased generation efficiencies and other capabilities [9]–[13]. If an EMS is interfaced with the commercial electricity grid and a microgrid, then it can improve electrical energy security and reduce electrical energy cost with enhanced energy management. A block diagram of an EMS interfaced with the commercial electricity grid and a microgrid is shown in Figure 2.

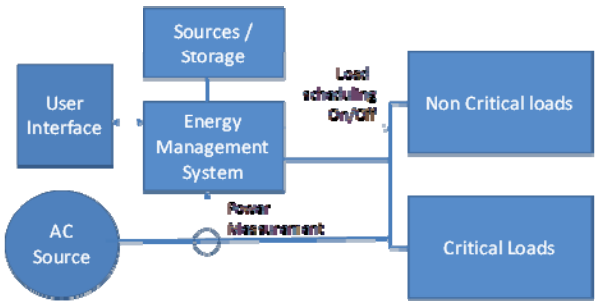

Figure 2. An EMS interfaced with the commercial electricity grid and a microgrid.

The energy security of DoD facilities can be improved and the energy cost reduced without re-design of the present transmission and distribution system. This can be done by breaking a facilities distribution system into multiple EMS controlled microgrids [5]. The capability of an EMS controlled microgrid to dynamically shift to autonomous operation provides DoD facilities with the ability to ride through commercial electricity grid power failures without an interruption in operations. In addition, an islanded EMS controlled microgrid can dynamically reduce the electrical load demand on the DR such that the facility can operate indefinitely without the commercial electricity grid. Lastly, an EMS controlled microgrid can perform DR power flow control in order to reduce or increase the percentage of DR power supplied to electrical loads. Microgrids operating in parallel with the commercial electricity grid can reduce or increase the electrical power demand on the commercial electricity grid when it is financially advantages. Making DoD facilities into multiple microgirds operating in parallel with the commercial electricity grid will improve energy security and reduce energy costs.

B. OBJECTIVE

A microgrid controlled by an EMS can optimize the use of DR to provide energy security and reduce energy costs. Specifically, an EMS can reduce a microgrid's peak power demand on the commercial electricity grid or on DR. The goal of this thesis is to investigate peak power demand of a microgrid and to perform peak power control using an EMS that reduces a microgrid's peak power demand such that energy security is improved and energy cost reduced.

C. APPROACH

The power demand of a potential microgrid was analyzed first. For this research a single family home power demand was monitored. Second, the EMS was modeled and experimentally verified using the circuit in Figure 3. Third, the validated model was used to investigate scenarios with more complex loads such as motors and diode rectifiers. Lastly, the model with the complex loads was simulated with and without the EMS.

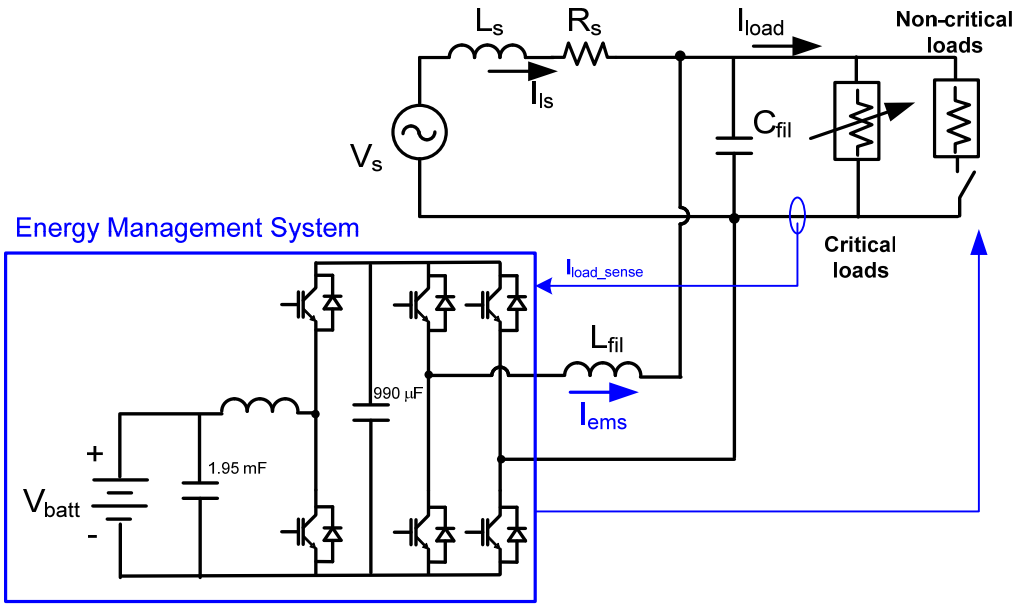

Figure 3. Circuit schematic used to experimentally verify the EMS model.

D. THESIS ORGANIZATION

The power demand profile of a single family home representing a microgrid and its loads are presented in Chapter II. Physics based modeling, computer simulation in Simulink, and experimental validation of the EMS is discussed in Chapter III. A description of the hardware, the control software design, the equipment setup and performance is also included in Chapter III. More complex scenarios are explored using the experimentally verified Simulink model in Chapter IV. Electrical loads common to a single family home or a DoD facility are modeled and simulated in Chapter IV. Conclusions and recommendations for future research are presented in Chapter V. The Matlab code used to simulate the model and to plot various figures in the thesis is included in the Appendix.

II. MICROGRID ANALYSIS

A. INTRODUCTION

A microgrid is an electrical power system that can operate independently or in parallel with the grid [3]. In this chapter, the structure of a microgrid is discussed, the power demand profile for a potential microgrid is analyzed and the operating patterns of some common loads are presented.

B. MICROGRID

The microgrid concept can be applied to any subsystem currently attached to the distribution grid. The size of the microgrid can vary. Multiple coordinating microgrids may be necessary to support a single building or one microgrid may be sufficient to support a single family home. In either case, each microgrid coupled with an EMS should be sized based off the critical loads it supports and the DR available to support those critical loads.

For the purposes of this research, a single family home was chosen to represent the loads of a potential microgrid. To apply the conclusions drawn from this approach to a larger building or multiple buildings, the power capability of the microgrid's DR would have to be increased or the building(s) would have to be broken down into multiple microgrids capable of coordinating together or operating independently to support all the critical loads.

A single family home electrical distribution system is illustrated in Figure 4. In a typical single family home, the load demand drives the current drawn from the commercial electricity grid. Distribution panel breakers only open if the current drawn exceeds the cable rating. The loads in the single family home are dependent on the power supplied by the commercial electricity grid.

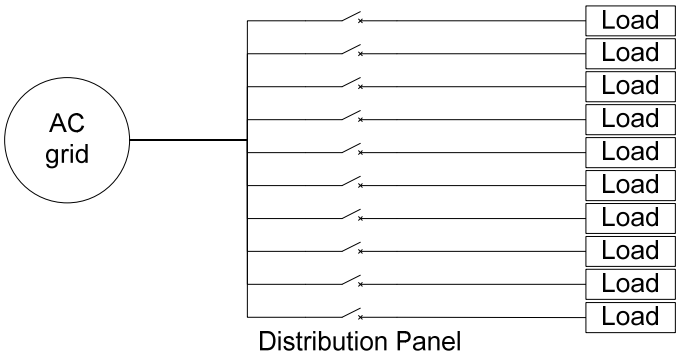

Figure 4. A single family home electrical distribution system.

A single family home as a microgrid with an integrated EMS is illustrated in Figure 5. The switches shown are used by the EMS to perform load shedding and islanding. The bi-directional power converter is used to decrease or increase the current drawn from the commercial electricity grid or to support the electrical loads while disconnected from the commercial electricity grid. The distribution panel breakers are not shown, but would be located downstream of the islanding switch and upstream of the EMS load switches. Large loads that may consume a single breaker on a distribution panel are shown as a single load in Figure 5 and can be individually turned off by the EMS.

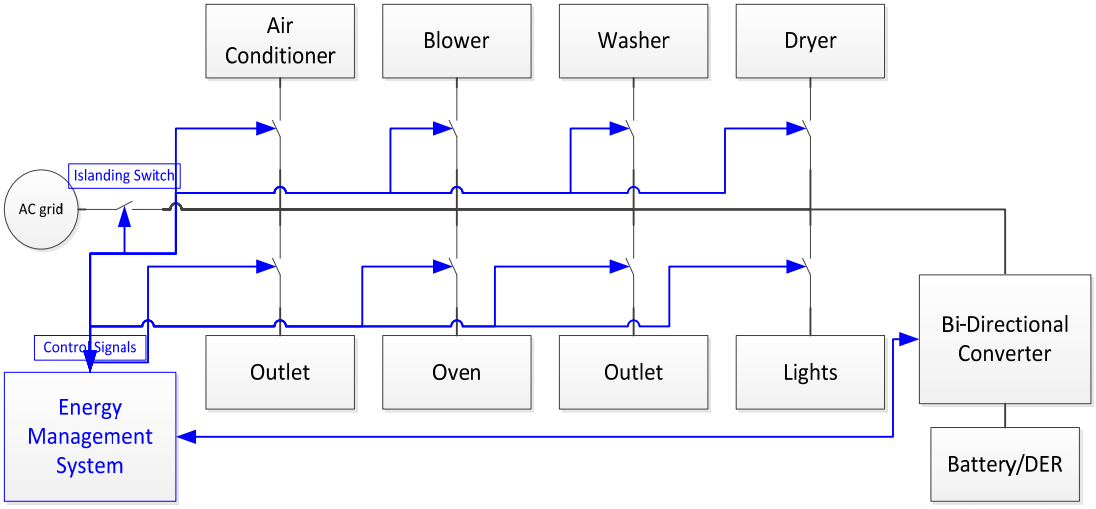

Figure 5. A single family home microgrid with an integrated EMS.

Loads designated as outlets or lighting in Figure 5 are smaller loads that can be supported by a single breaker. Loads that may be powered from the switch supplying the outlet load seen in Figure 5 are illustrated in Figure 6. These loads are emphasized because they cannot be considered controllable loads and have the ability to place a large power demand on the system. The EMS must shed all of the loads seen in Figure 6 if load shedding of the outlet is required. Additionally, if the EMS restores this switch, the same loads may start up immediately. This could cause an inrush current that results in another load shedding event. This cycle could repeat indefinitely without user intervention if the correct system logic is not implemented to ensure load oscillations such as this do not occur. Load oscillations are discussed further in Chapter IV.

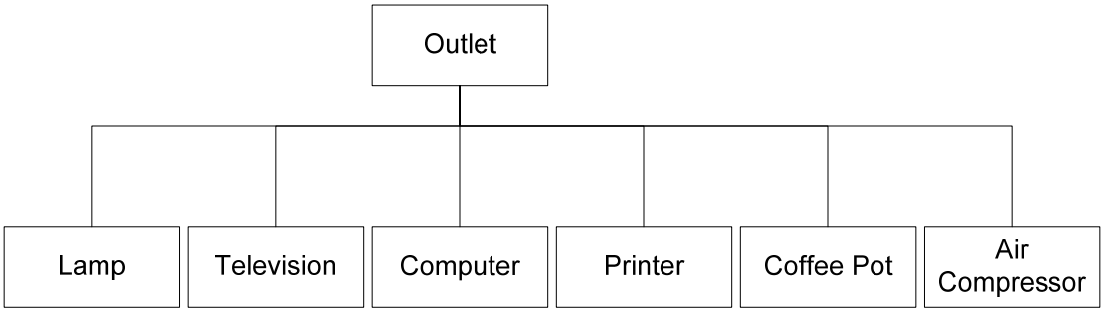

Figure 6. Plug-in loads that an EMS cannot control directly.

C. POWER DEMAND PROFILE OF A SINGLE FAMILY HOME

1. Average Daily Power Demand Profile of a Single Family Home

The power demand profile of a single family home was analyzed. The single family home data was retrieved from the Pacific Gas and Electric (PG&E) smart meter readings available online to all customers. The annual hourly power usage $P_{kW\text{-}hour}$ is given by

$$P_{kW-hour,\,annual\ average} = \frac{1}{365}\sum_{d=1}^{365} P_{kW-hour} \tag{1}$$

and is used to calculate the average of the real power $P_{kW\text{-}hour,\,annual\ average}$ consumed during that hour daily. The average hourly values are then given by

$$P_{kW-hour,\,average} = \frac{1}{24}\sum_{hour=1}^{24} P_{kW-hour,annual-average} \tag{2}$$

to find the annual average power consumed per hour over 24 hours $P_{kW\text{-}hour,\,average}$.

The results are shown in Figure 7. The lines are only used to connect the data points together. The daily peak power demand of a single family home is illustrated in Figure 7. The home uses approximately 300 W during low power demand times and approximately 1.2 kW during peak power demand times on average. That is approximately four times as much power required during the peak power demand time. A similar power profile exists for every household. The minimum and maximum values will vary based on location and household usage, but the shape remains similar [14]. The peak power demand is what drives the generating capacity of the commercial electricity grid [14]. More specifically, about 20% of electrical generating capacity exists to meet peak power demand 5% of the time [3]. This requires the power utilities to keep generating capacity in reserve [3].

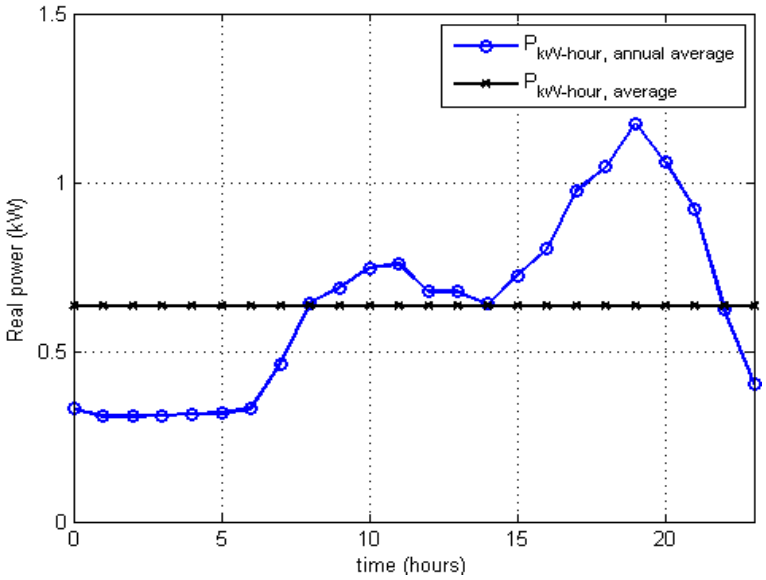

Figure 7. A single family home average daily power demand.

The annual average hourly power, 650 W, demanded by this home is shown in Figure 7 as well. The power consumed by the home for both curves remains the same;

however, the power required at any moment in time is significantly reduced by decreasing the peak power demanded and increasing the low power demand. In order to have this type of power demand profile a combination of DR and load management is necessary.

Facilities that support DoD operations will have a different power demand profile than seen in a single family home but will still have peak power demand and low power demand. An EMS altered to accommodate the critical and non-critical load demands of DoD facilities could reduce the peak power demanded by those facilities. This would enhance energy security and reduce energy costs without requiring significant changes to the present distribution system.

2. Daily Power Demand Profile of a Single Family Home

The power demand profile of the single family home discussed in Chapter II.C.1 was recorded over a twenty-four hour period. The measured real power, reactive power, and apparent power demanded by the home are illustrated in Figure 8. The data was recorded using a Fluke 434 Power Meter. Data points were recorded at 30 s intervals. The lines in the plot connect the data points.

The power demand profile shown in Figure 8 is slightly different then the power demand profile seen in Figure 7. The drastic changes in power demand are more clearly shown in Figure 8 than Figure 7. Multiple times during the day, the power demand went from between five and six kW to less than one kW. In most cases, these changes are the result of a single large load running. While the exact loads running during the peak power demands seen in Figure 8 are unknown, other measurements taken of loads operating in the home indicate that the peak power demands are due to the dryer and washer running cycles and/or the oven operating. As stated before, the peak power demanded from the commercial electricity grid can be reduced by supplementing it with energy from DR or by load shedding. During low power demand times energy from distributed generators (DG) can provide power to the operating loads or energy from the commercial electricity grid can provide power to the operating loads and charge batteries in order to maintain a constant power demand on the commercial electricity grid.

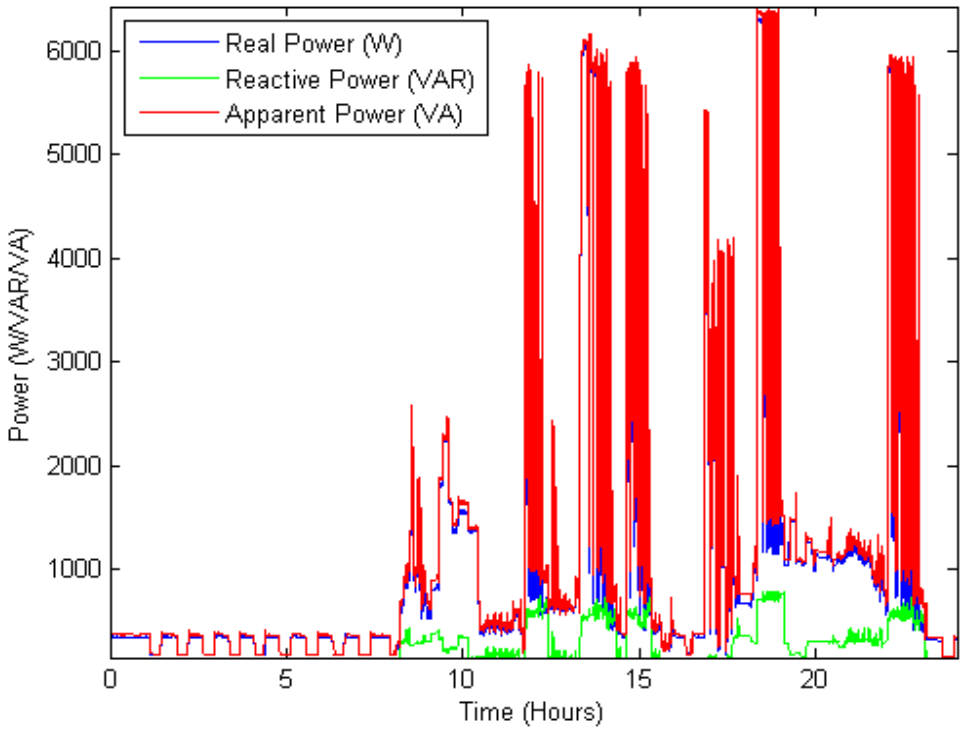

Figure 8. Single family home power demand profile recorded on 9/12/2012.

The current demand profile from the same data seen in Figure 8 is shown in Figure 9. The lines in the plot connect the data points. The profiles are identical in shape and differ only in magnitude. Since the home is powered from the commercial electricity grid, it is safe to assume the voltage is a constant 120 V. The commercial electricity grid current can be used in conjunction with the homes load current and an EMS current to make logic decisions concerning peak power control. Specifically, the EMS can determine if it should provide supplemental current to reduce the current demand on the commercial electricity grid, shed loads to reduce the load current demand and the current demand on the commercial electricity grid, or increase the current demand on the commercial electricity grid by charging batteries.

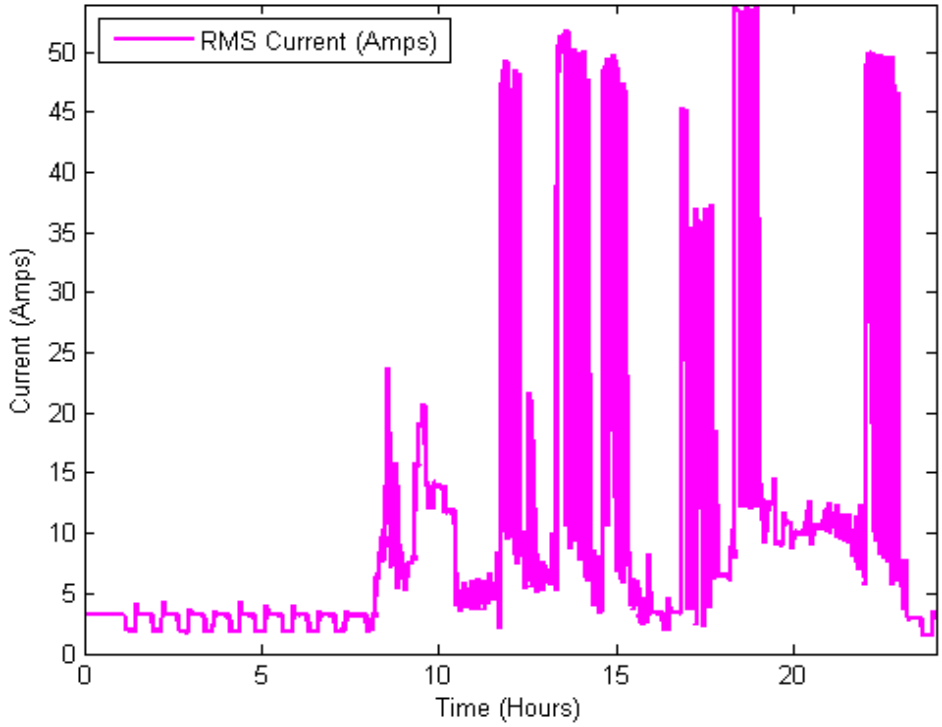

Figure 9. Single family home current demand profile recorded on 9/12/2012.

3. Individual Load Power Demand Profiles

The power demand profiles of individual loads were recorded using a Fluke 434 Power Meter. This was done to identify what loads were driving peak power demand and to identify cyclic loads whose operation could be delayed. Multiple recording modes and trials were done on each load to understand the general operating pattern and the power demand. The clearest description of the loads analyzed operating patterns are shown in Figures 10 through 15.

The operating pattern of the clothes dryer is illustrated in Figure 10. The lines in the plot connect the data points. The data points were recorded at one second intervals. The voltage is an average of the separate line voltages supplied to the dryer. The current is the summation of the separate currents drawn by the dryer. The operating pattern displays the cyclic nature of the dryer and its high energy demand. The power demanded by the dryer creates the peak power conditions seen in Figure 8 and Figure 9. The real and the reactive power drawn by the dryer is displayed in Figures 11 and 12 for comparison with Figure 8.

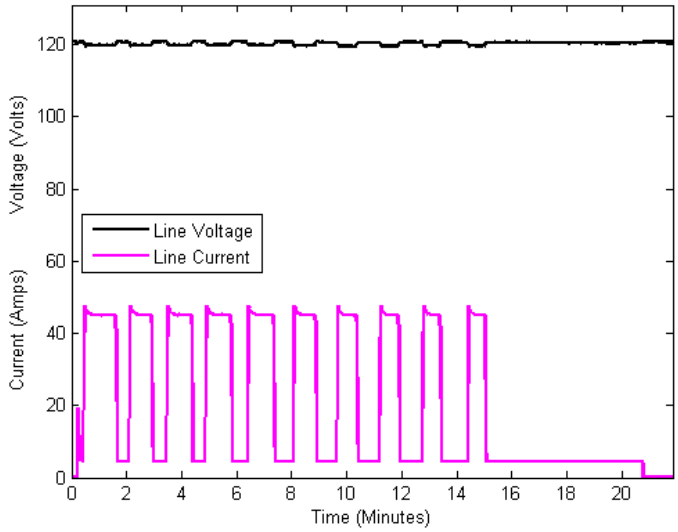

Figure 10. The current and voltage demand of the clothes dryer.

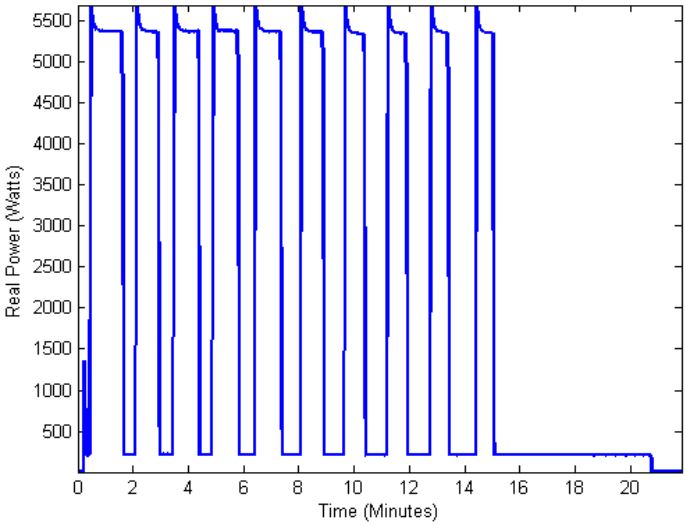

Figure 11. The real power demand of the clothes dryer.

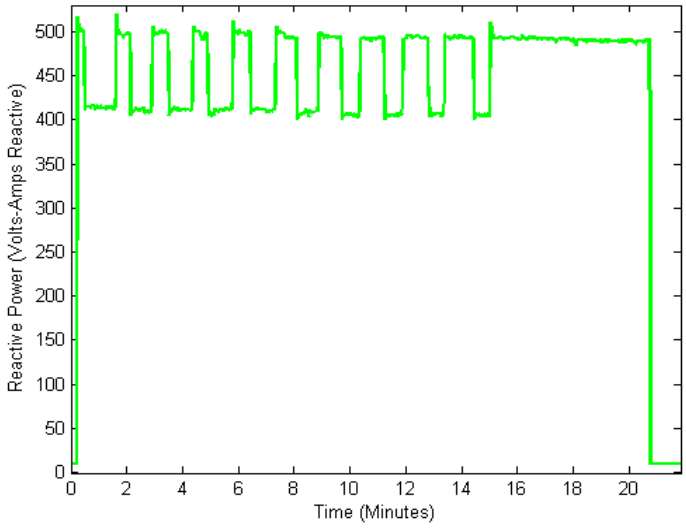

Figure 12. The reactive power demand of the clothes dryer.

The operating pattern of a refrigerator can be seen in the bottom left of Figure 8 from midnight to seven. A close up of the rms current drawn by the refrigerator is displayed in Figure 13. The lines connect the data points. Data points are recorded every five seconds. The current demanded by the refrigerator is not significant when compared to the dryer, but both loads have cyclic operating patterns. The refrigerator turns on and off for longer periods of time than the dryer.

The operating pattern of a coffee pot is illustrated in Figure 14. The lines connect the data points. Data points are recorded every second. The rms current drawn by a coffee pot is shown in Figure 14.

The operating patterns of the dryer, refrigerator, and coffee pot are all cyclic and predictable to a certain extent. Their operation can be delayed for a reasonable amount of time or other loads can be shed temporarily while they turn on. The advantages and disadvantages of load shedding while higher priority loads operate in order to minimize peak power demand is discussed in Chapter IV.

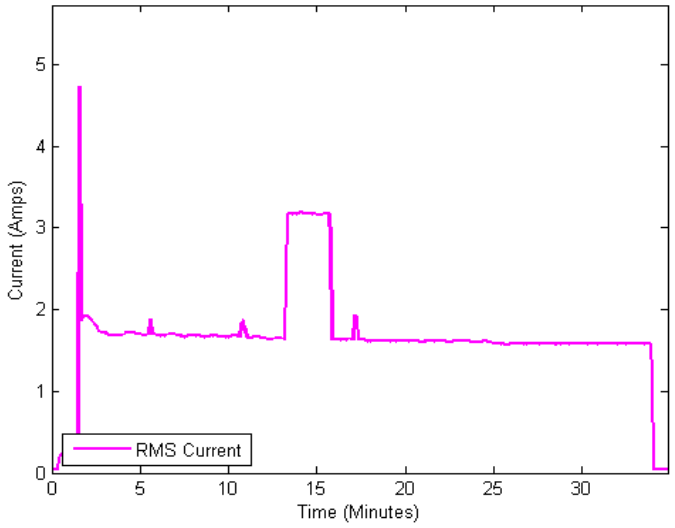

Figure 13. An "on" cycle for a refrigerator.

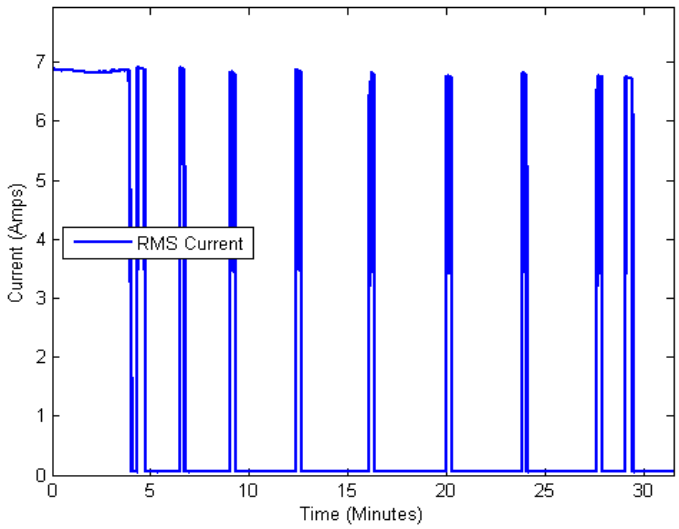

Figure 14. Operating pattern of a coffee pot.

D. CHAPTER SUMMARY

In this chapter, the structure of microgrids was discussed, and a single family home electrical power demand was analyzed. Loads with cyclic operating patterns whose operation can be delayed or result in load shedding were discussed. In the next chapter, the Simulink model of the EMS controlled microgrid and experimental results are presented.

III. EMS CONTROLLED MICROGRID MODEL AND EXPERIMENTAL RESULTS

A. INTRODUCTION

In this chapter, the EMS functionality, Simulink model, and hardware are presented in detail. The functional objectives of the EMS are addressed first. The Simulink model and the circuit it represents are then covered. Third, the EMS hardware and software are presented, and lastly, the experimental results confirming the validity of the Simulink model are discussed.

B. EMS FUNCTIONALITY

The EMS creates the opportunity to manipulate power intelligently in a microgrid. Its functionality is demonstrated by modeling, simulation and experimental validation of the following scenarios:

1) Peak power control by tapping an energy storage system during high demand.

2) Islanding mode by necessity (loss of power) or by choice.

3) Peak power control by non-critical load shedding during transients.

By functionally supporting the above scenarios, the EMS can be very useful in commercial electricity grid connected systems where there is a limit on the user's power consumption. If the EMS keeps the commercial electricity grid current, or the main power source current, below a set threshold at all times with supplemental current and load management or shedding, then the user can operate loads beyond the steady-state power limits without worrying about the circuit breaker interrupting service. The EMS can also be useful when the user pays different rates for power delivered at different times of the day. In this case, the EMS can manage the energy stored and energy drawn from the commercial electricity grid to reduce consumption when the power rates are higher.

Three scenarios are illustrated in Figure 15 where a microgrid with a single-phase main power source and a battery pack is used to demonstrate the functionality of the EMS [15]. The battery pack can be recharged from the grid or from DR such as PV cells, etc. Two sets of loads, one critical and the other non-critical, are used to demonstrate the EMS functionality. The first scenario, illustrated in the bottom left of Figure 15, demonstrates how the peak rms current drawn from the source is limited by the EMS when the critical load increases. The EMS behaves as a current source, providing supplemental current demanded by the loads and reducing the current demand on the main power source. The second scenario, illustrated in the bottom right of Figure 15, demonstrates islanding mode of operation. Islanding of the microgrid can occur when the load is so light that the battery, or stored energy, can provide all its current or when there is a fault or poor power quality in the main power source. In the second scenario, the EMS inverter operates as a voltage source. The third scenario, illustrated in the top right of Figure 15, demonstrates how the EMS can shed a non-critical load when the critical load increases, thus keeping the main power source rms current below a set threshold. In the third scenario the EMS first provides supplemental current to reduce the main power source rms current and then sheds non-critical loads to maintain the main power source rms current below the set threshold.

The EMS control algorithm was developed with the following goals, listed here in order of priority:

1) Power must be available to the critical loads at all times. As an example, if the main power supply (commercial electricity grid) is down, then battery power will be used to support critical load operation.

2) Reduce the peak power demand of the microgrid on the main power source by using battery power and by non-critical load shedding.

3) Maximize the state of charge of the battery.

4) Make power available to non-critical loads.

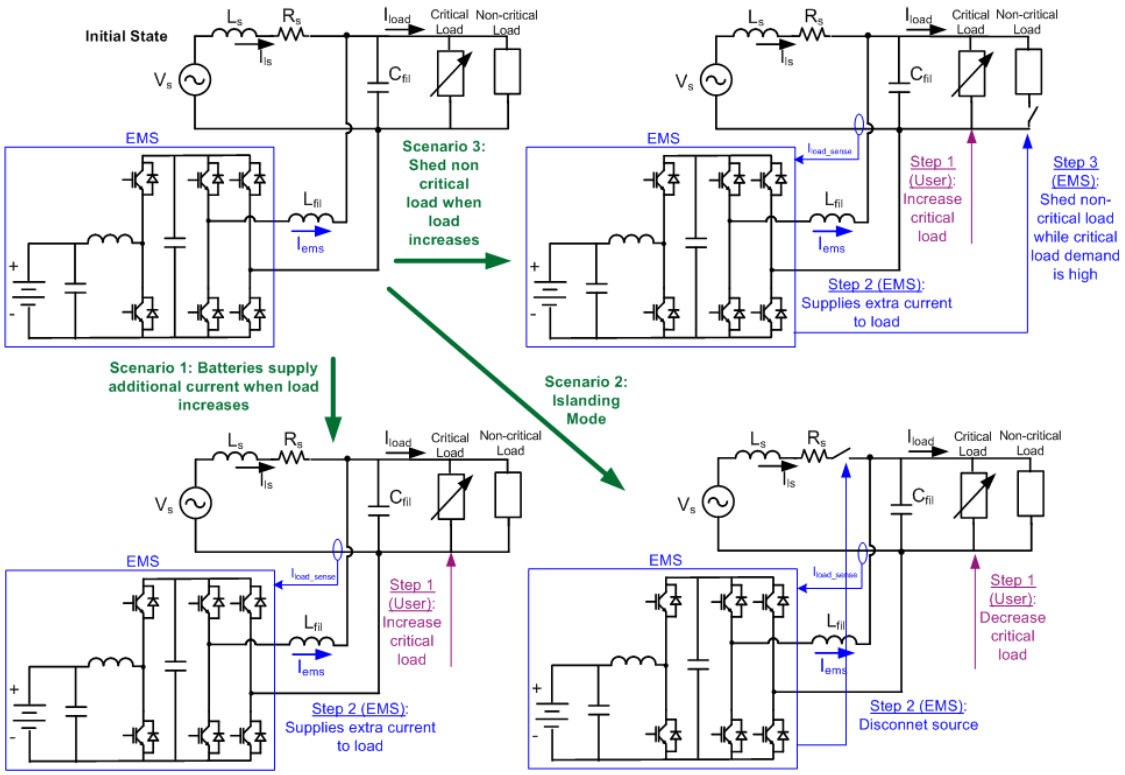

Figure 15. The scenarios used to demonstrate EMS functionality.

C. EMS MODELING

1. Simulink Model, Circuit Schematic and rms Computation

A physics based model of the EMS was developed and implemented using Simulink software [16]. The top level Simulink model block diagram including the EMS, critical and non-critical loads, and the main power source are shown in Figure 16. The circuit schematic of the Simulink model is shown in Figure 17.

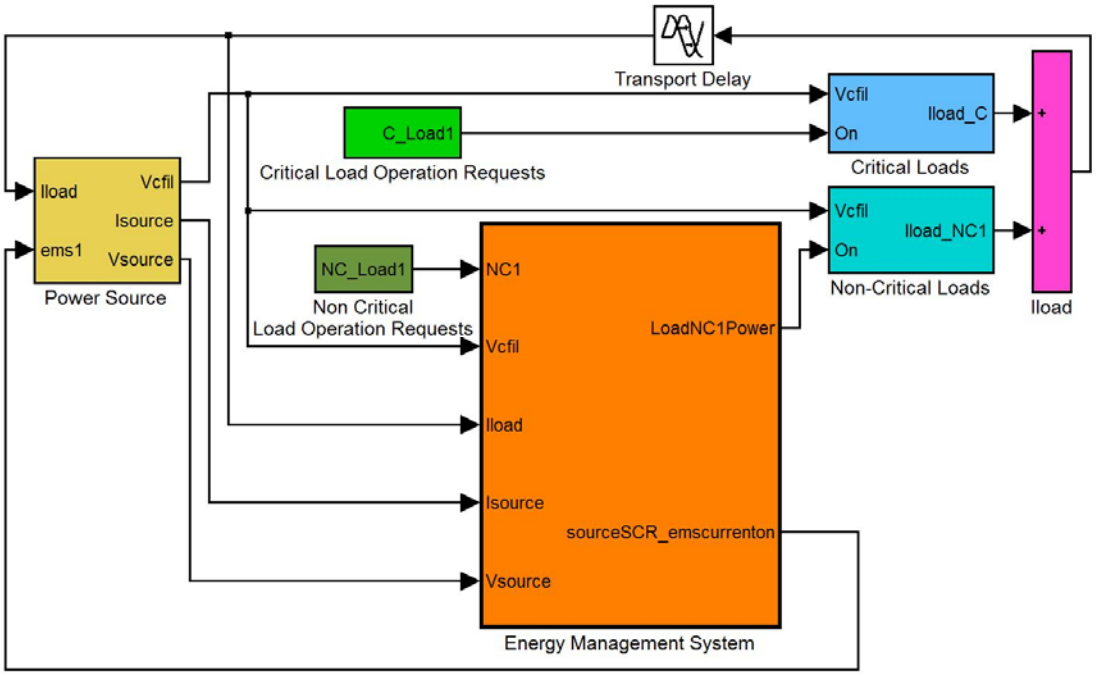

Figure 16. The physics based Simulink model block diagram of the EMS.

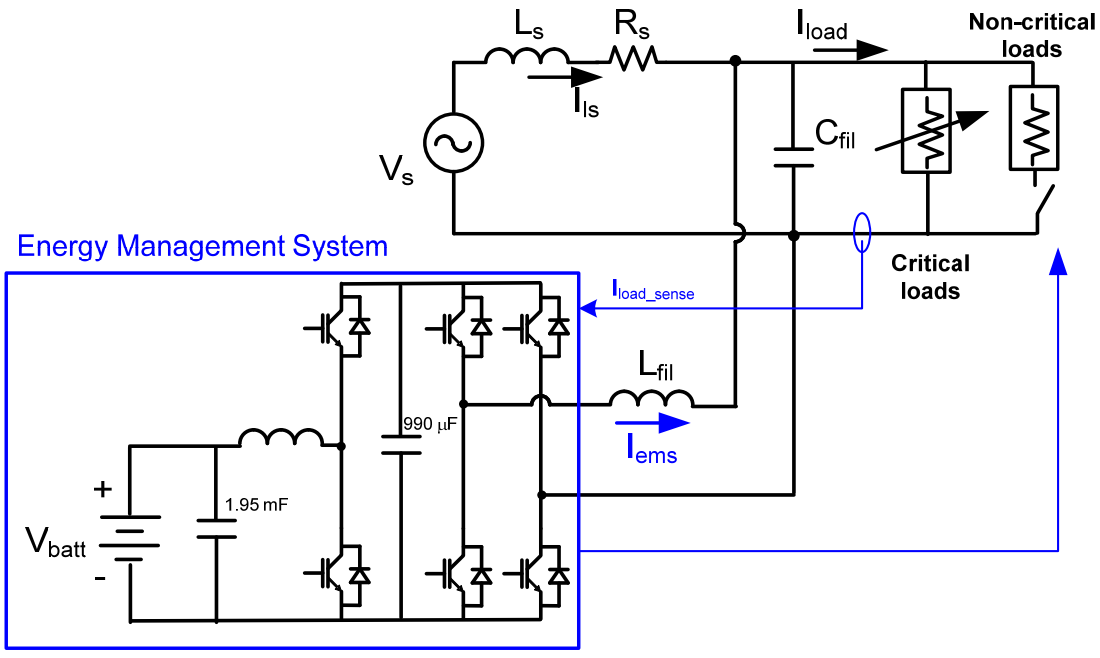

Figure 17. Circuit schematic implemented in the Simulink model.

The EMS block in Figure 16 includes the logic algorithm which controls the loads intelligently. The logic algorithm, seen in Figure 19, is implemented using a Matlab

function block. The load current, the status of the non-critical load, the availability of the main power source and a disable/clear pushbutton toggle are inputs to the Matlab function block. The Matlab function block outputs the signals that allow the EMS to provide stored energy as a current source or voltage source and to shed or restore non-critical loads.

The Matlab function block uses the rms value of the load current and the source voltage. The rms values of these signals are calculated in the EMS block and are given by

$$I_{rms} = I_{avg} \frac{\pi}{2\sqrt{2}} \tag{3}$$

where I_{avg} is the average current. In Equation (3), the relationship

$$I_{rms} = I_P / \sqrt{2} \tag{4}$$

$$I_{avg} = \frac{2I_p}{\pi} \tag{5}$$

is used, where I_p is the peak current for a sinusoidal current. Equation (5) is applicable to a rectified sine wave whose average value I_{avg} is given by

$$I_{avg} = \frac{2}{T} \int_0^{T/2} I_p \sin(\omega t)\, dt = \frac{2I_p}{\pi} \tag{6}$$

where $w = 2\pi / T$.

The Simulink model determines the average value by taking the absolute value of the input and sending it through two 5.0 Hz low pass filters as seen in Figure 18. The transfer function of the low pass filter is

$$H(s) = \frac{w_c}{s + w_c} \tag{7}$$

where w_c is the low pass filter cutoff frequency. The average value I_{avg} is then multiplied by the constant in (3) to obtain the rms value I_{rms}.

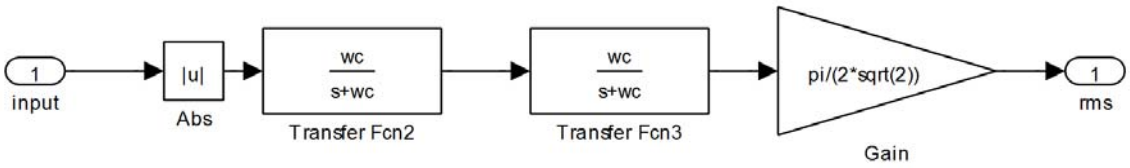

Figure 18. The RMS computation block diagram.

2. EMS Control Logic

The control logic used to draw supplemental current from the battery, to island the microgrid from the main power source, or to perform load shedding is performed in the Matlab function block. The function coding is listed in Section A of the Appendix.

The logic used to determine if supplemental current should be provided from the battery compares the load current I_{load} to two thresholds, $I_{ems\text{-}on}$ and $I_{ems\text{-}off}$. The value that the load current I_{load} must be greater than to turn on supplemental current is $I_{ems\text{-}on}$. The value that the load current I_{load} must be less than to turn off supplemental current is $I_{ems\text{-}off}$. The two values to turn on and to turn off supplemental current are necessary because the rms value for the load current I_{load} is a sinusoidal value, and using a single value for both decisions could result in the supplemental current oscillating on and off. Supplemental current logic is bypassed when the microgrid is islanded because the battery is providing all the power to the critical loads.

The logic used to determine if the main power source is available is a relational operator block or a comparator. The rms voltage on the main power source is compared to a constant value of 100 V. If the rms voltage is less 100 V, then the source is lost and the EMS will disconnect from the main power source, or island, and provide power from the battery to the loads.

The peak power control load shedding logic is shown in Figure 19 for the single non-critical load circuit illustrated in Figure 17. The logic is dependent on the status of the main power source, the load current, the status of the non-critical loads and a load shedding disable/clear pushbutton toggle. The value of the load current threshold to shed non-critical loads depends on whether the microgrid is connected to the main power source or islanded. The load current threshold to shed non-critical loads is referred to as

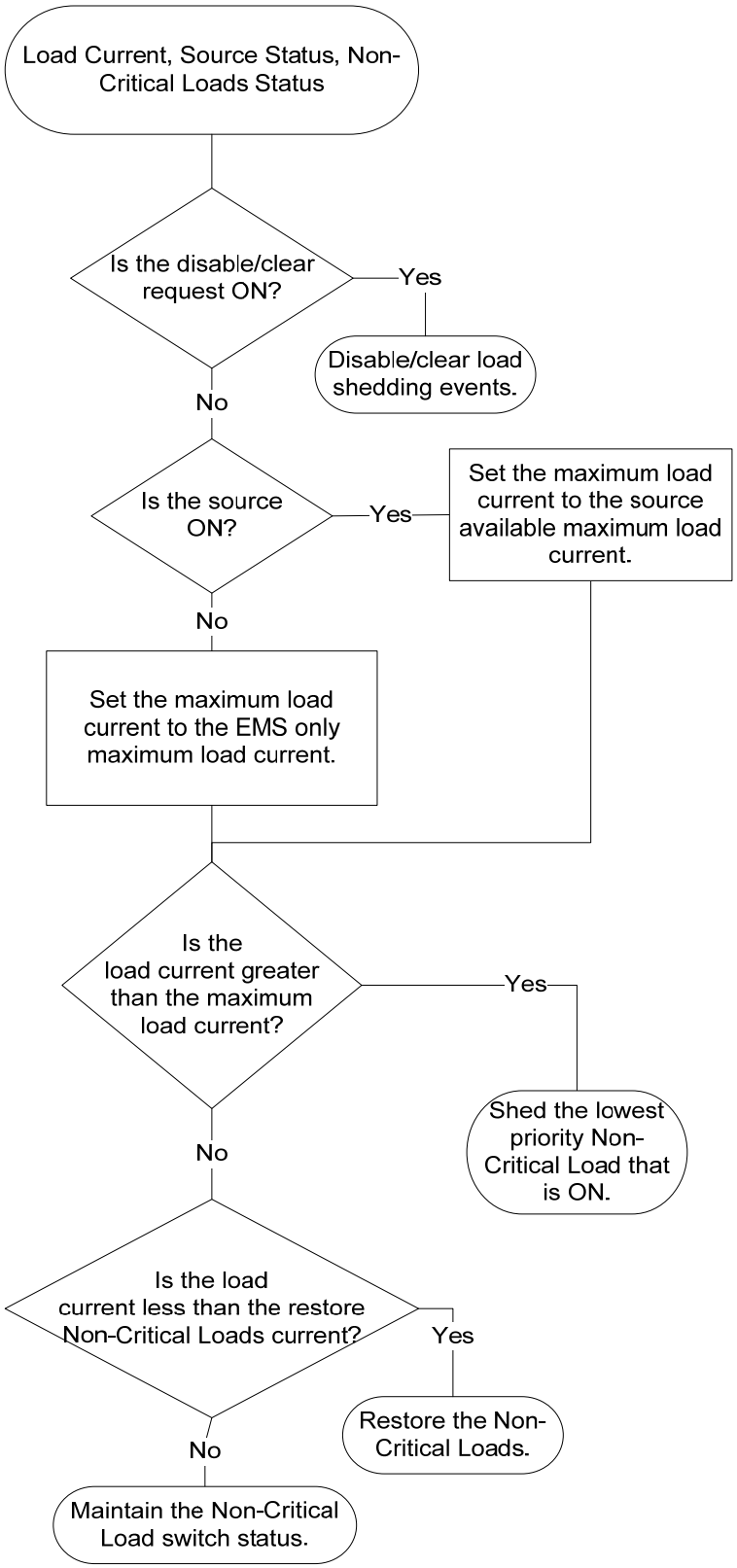

Figure 19. The EMS load shedding control logic.

I_{max}. If the main power source is not available due to a fault, then I_{max} is set to a lower value to support sustained islanding operations. If the main power source is connected to the microgrid, then I_{max} is set to a higher value that supports peak power control. The same approach is used for the load current restoration threshold I_{maxoff}, which is used to restore non-critical loads that have been shed. If the main power source is not available, then I_{maxoff} is set to a lower value than if the source is powering the microgrid, similar to what was done with I_{max}.

When the main power source is available, I_{max} is set to provide supplemental current from the battery prior to shedding any non-critical loads. If at any time the load current is between I_{max} and I_{maxoff}, the EMS maintains the non-critical loads' previous switch state.

The disable/clear push button toggle input is also incorporated into the load shedding logic. This allows a user to disable the load shedding capability or to clear a load shedding transient that did not restore the non-critical loads because the load current did not fall below the I_{maxoff} threshold.

3. Critical and Non-critical Load Blocks

The critical load and non-critical load blocks seen in Figure 16 are nearly identical in implementation. The non-critical load block implementation is shown in Figure 20. The two blocks use different resistive values, and the critical load block is made up of three resistive loads. The first input to both blocks is the voltage across the load V_{cfil}. The second input is the on/off signal. In the case of the critical load, the on/off signal is three multiplexed signals, one for each resistive load. The output from each block is the current through the load. The output of the blocks is computed using

$$I_{load} = V_{cfil} / R \tag{8}$$

where R is the resistance of the load.

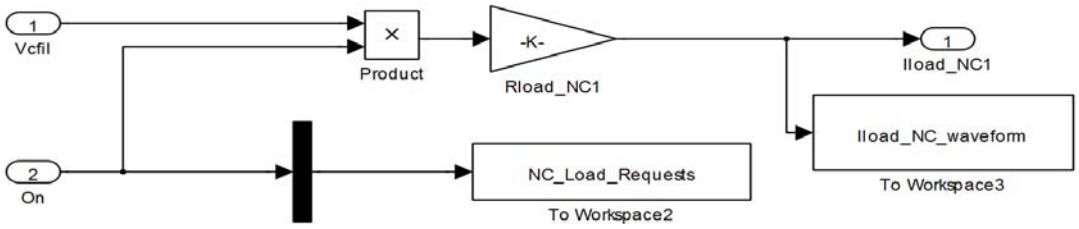

Figure 20. The non-critical load block implementation.

4. Power Source Block

The power source block in the Simulink model represents the commercial electricity grid and is referred to as the main power source. It implements the following differential equations with respect to Figure 17:

$$V_{source} - sL_s I_{source} - R_s I_{source} - V_{cfil} = 0 \tag{9}$$

$$I_{source} = \frac{1}{sL_s}\left(V_{source} - V_{cfil} - R_s I_{source}\right) \tag{10}$$

$$I_{cfil} = I_{source} - I_{load} + I_{ems} \tag{11}$$

$$V_{cfil} = \frac{1}{sC_{cfil}} I_{cfil} = \frac{1}{sC_{cfil}}\left(I_{source} - I_{load} + I_{ems}\right) \tag{12}$$

where *s* represents differentiation in (9)-(12).

The supplemental current from the battery is called the EMS current I_{ems}. The EMS current I_{ems} is implemented in the EMS block. It is implemented using an H-bridge model and is regulated using a proportional-integral (PI) controller to maintain the relationship $I_{ems} = I_{load}/2$ [17]. The output of the H-bridge model is a DC voltage V_{dc} that switches between positive, zero, and negative 200 Vdc. The EMS current I_{ems} is found with

$$I_{ems} = \frac{1}{sL_{fil}}\left(V_{dc} - V_{cfil}\right) \tag{13}$$

where V_{dc} is the switching DC voltage output from the H-bridge.

D. EMS HARDWARE

The power electronics based power conversion system shown in Figure 21 and Figure 22 was designed to support laboratory development and rapid experimental validation for research and thesis projects [18]–[21]. It includes a field programmable gate array (FPGA) development board [22] with input/output (I/O) ports, an insulated gate bipolar transistor (IGBT) power module, power supply, voltage/current sensors, analog/digital (A/D) converters, transistor-transistor logic (TTL) interface and a USB interface to communicate with a personal computer (PC) as shown in the schematic of Figure 21. A Joint Test Action Group (JTAG or IEEE Standard 1149.1) programming cable interfaces the FPGA development board to a PC and is used to program the FPGA. The software development tool used for the FPGA is Simulink [16] with the addition of Xilinx System Generator software [23] which compiles the Simulink model to create VHDL code. The interface functionality of Figure 21 is realized by two printed circuit boards (PCBs) mounted above and below the FPGA development board as shown in Figure 22. The bottom PCB includes the power components such as the IGBT Integrated Power Module (IPM), current and voltage sensors, passive components and DC power supply. The IGBT IPM includes six diodes, six IGBTs and the gate drive circuits in the standard three phase-three legs configuration. For the EMS presented in this thesis, two legs are used in a single-phase H-bridge inverter configuration, while the third leg is used to interface with the battery pack. The PCB mounted on top of the FPGA development board includes a USB interface chip, USB connector to interface with the PC, A/D converters, voltage level shifters and several other connectors to interface with the other boards.

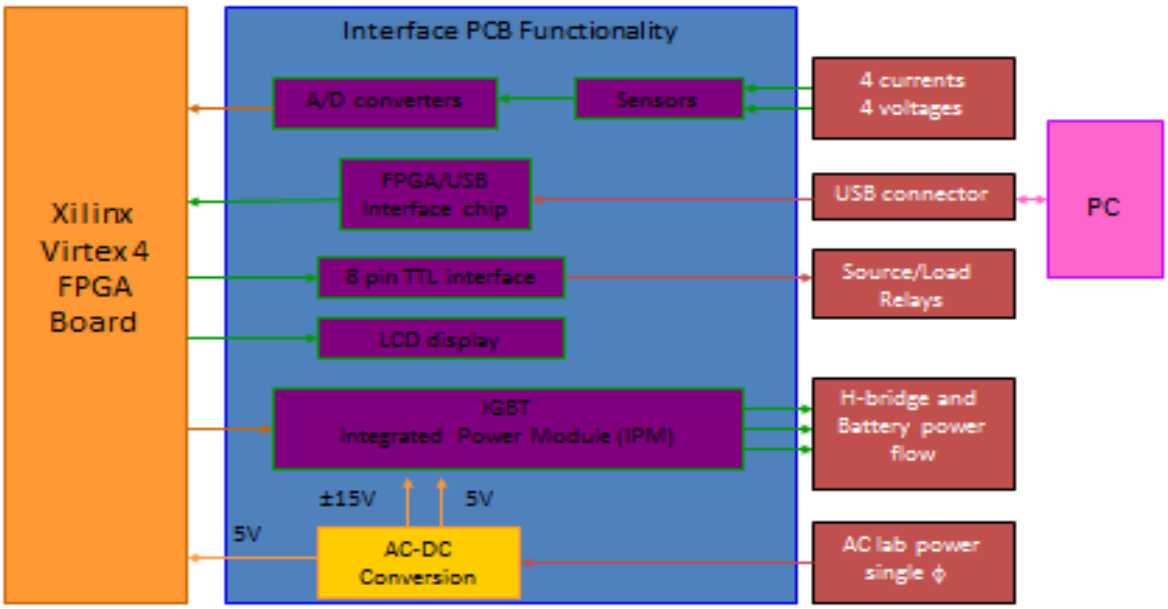

Figure 21. The EMS electronics block diagram.

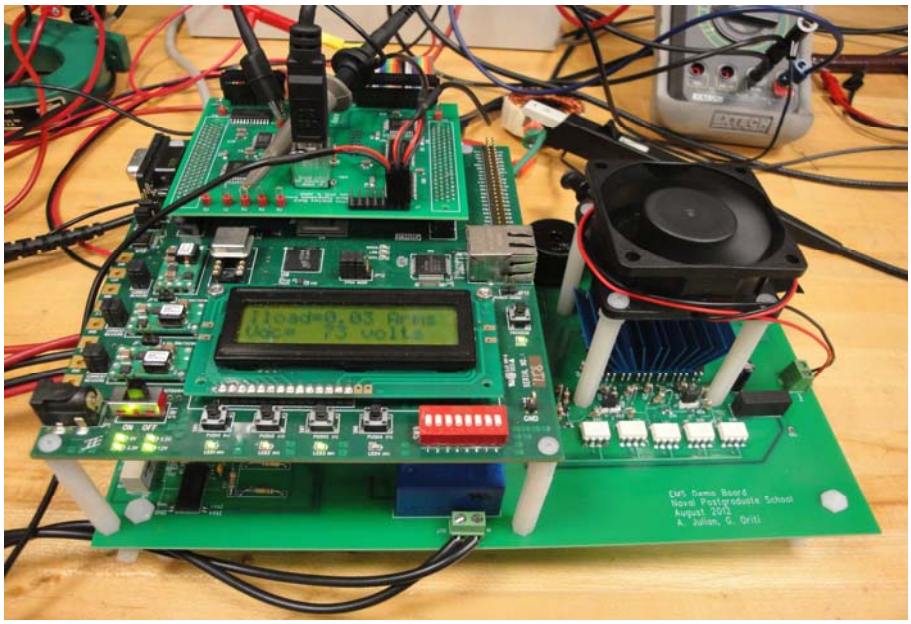

Figure 22. The FPGA based EMS electronics.

E. EMS SOFTWARE

The Simulink top level block diagram of the EMS software is shown in Figure 23. The voltage and current sensor inputs are read in via the A/D conversion blocks on the lower left of Figure 23. The voltage A/D conversion block provides the DC bus voltage and the AC source voltage to the Controller 1 block. The DC bus voltage or DC-Link voltage V_{dc} is the voltage across the 990 μF capacitor seen in Figure 17. The current A/D conversion block provides the DC current from the battery pack, the EMS current I_{ems} and the load current I_{load} to the Controller 1 block.

Signals to silicon controlled rectifier (SCR) relay switches used to perform load shedding and to island or reconnect the microgrid are output from the FPGA via the relay control block and the eight pin TTL interface.

The Chipscope interface block was used to interface the Chipscope program run on the PC with the EMS software [24]. The Chipscope software has a user interface that allows the user to provide inputs to the software via a USB cable. The Chipscope software and its interface were used for testing and to establish initial conditions for the experiments. The SCR relay switches for the non-critical load and for islanding could be directly controlled from Chipscope. The supplemental EMS current could be turned on and off from Chipscope as well.

The data recorder block can be used to record data via the USB cable connecting the EMS and the PC. It was not used in this thesis.

The Controller 1 block determines and carries out the logic decisions of the EMS. The block diagram of Controller 1 can be seen in Figure 24. The rms values of the load current I_{load}, the EMS supplemental current I_{ems} and the main power source voltage are calculated in the three green blocks annotated as rms computation. The rms values are determined using the same method discussed in the Simulink model. The rms computation block diagram is shown in Figure 25.

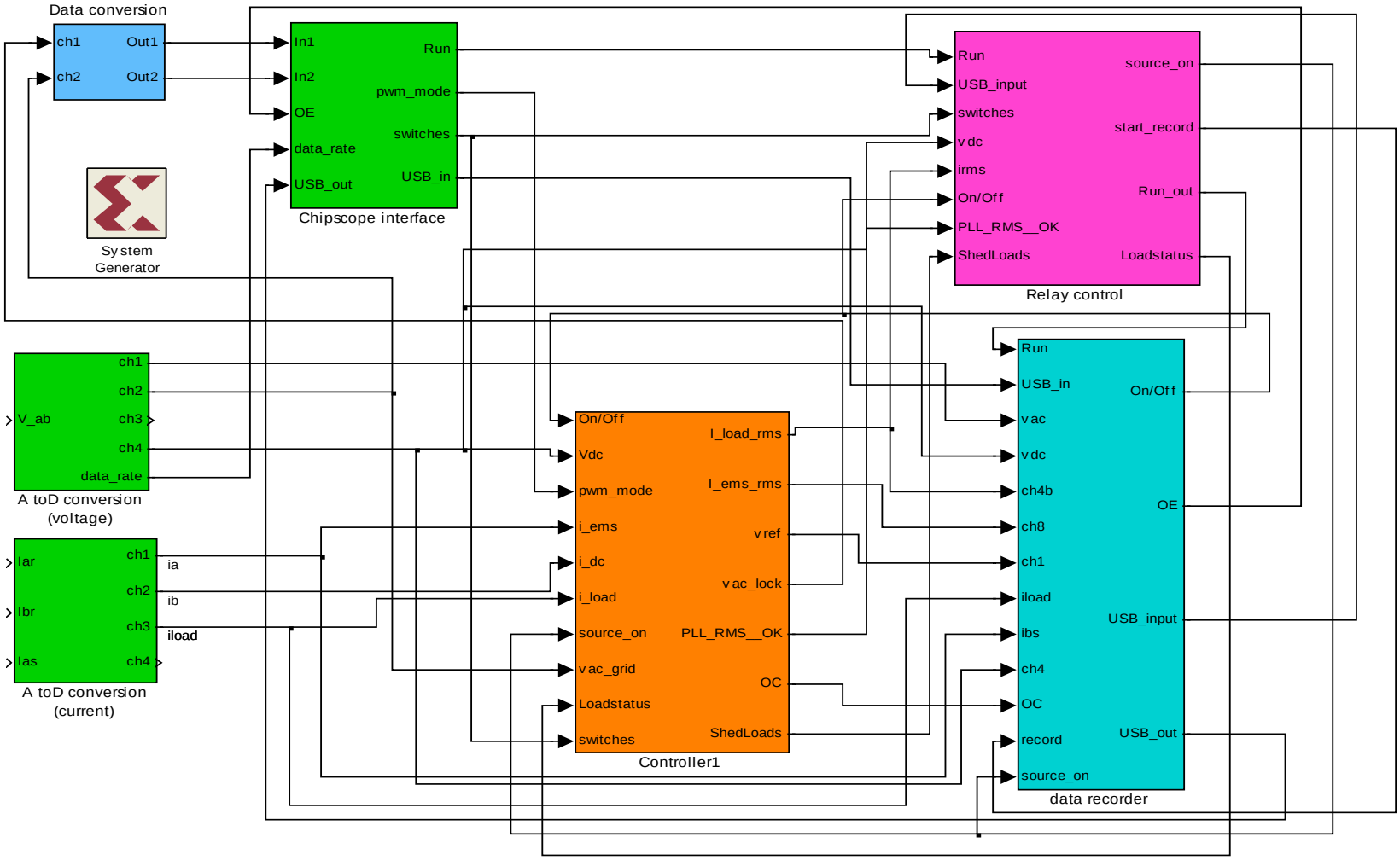

Figure 23. EMS software top level block diagram.

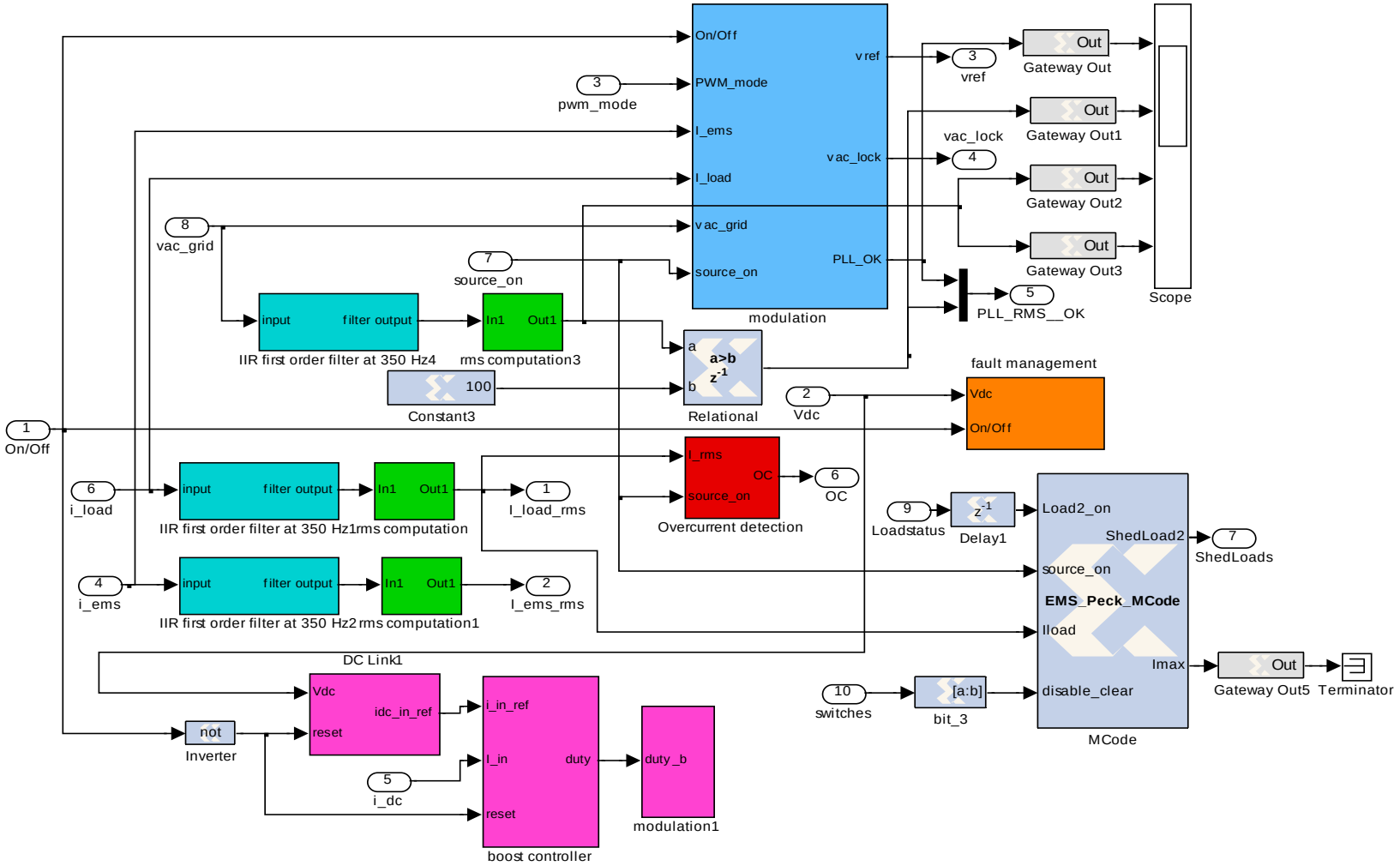

Figure 24. EMS software Controller 1 block diagram.

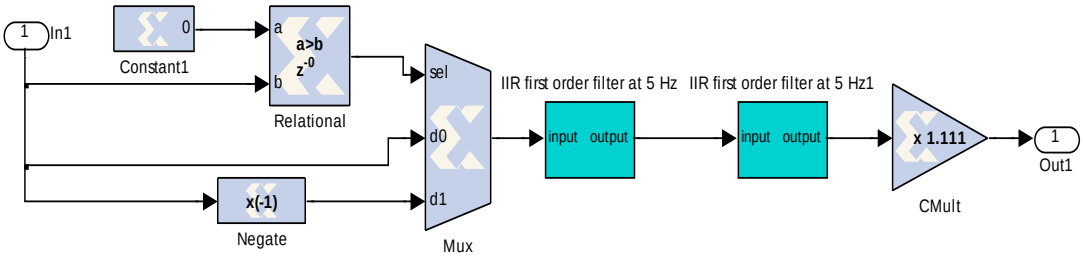

Figure 25. Block diagram of the rms computation block.

The decision to provide EMS current from the battery is done in the red overcurrent detection block, where the rms value of I_{load} is compared to a constant to determine if it is above or below the thresholds $I_{ems\text{-}on}$ and $I_{ems\text{-}off}$, respectively. If I_{load} is above $I_{ems\text{-}on}$ and the main power source is available, then EMS current I_{ems} is provided. If I_{load} is below $I_{ems\text{-}off}$ and the main power source is available, then I_{ems} is secured. If the main power source is not available, then this feature is disabled.

The decisions to shed loads or restore loads that have been shed are performed in the Xilinx block annotated MCode located in the bottom right of Figure 24 and a function similar to that produced for the Simulink model is used. The code for the MCode function is in Section A of the Appendix. The output of the MCode block controls a SCR relay that disconnects or connects the non-critical load to the circuit.

The Xilinx Relational block located in the center of Figure 24 compares the main power source voltage to a constant, 100 V, to determine if the main power source is available to supply power to the microgrid. The status of the main power source is then fed into the EMS current logic and used to disable it if the main power source is not available. The status of the main power source is also fed into the blue modulation block in Figure 24 where it is used to determine which reference value will modulate the H-bridge DC-AC inverter that makes up the second and third leg of the IGBT IPM. If the source is available, the reference comes from a PI controller that modulates the EMS current to maintain the relationship $I_{ems} = I_{load}/2$. If the source is lost, the reference is generated to maintain the capacitor C_{fil} voltage V_{cfil} at 110 V. The pulse width

modulation (PWM) mode for the DC-AC Inverter can be changed between bipolar and unipolar PWM using the Chipscope interface [25].

The voltage on the DC-link V_{dc} between the boost converter and the DC-AC inverter, as seen in Figure 17, is maintained at 200 V. A PI controller in the magenta block annotated DC Link1 determines the reference DC current needed to maintain 200 V. The reference DC current is fed into a PI controller in the magenta boost controller block, where it is compared to the actual DC current. The boost controller block outputs the control signal used to perform PWM. The modulation1 block compares a saw tooth signal to the control signal and outputs the gate control signals for the lower IGBT in the first leg of the IGBT IPM [25]. The boost converter is not bi-directional at this time and the top IGBT is kept off during all operation.

F. EMS EXPERIMENTAL RESULTS

1. Setup

The EMS was set up in the lab using the hardware described in Chapter III.D. The circuit shown in Figure 17 was simulated using the Simulink model and validated in the lab. The source voltage V_s was 120 Vrms, the battery pack voltage V_{batt} was 72 Vdc and was boosted to create a 200 Vdc bus V_{dc} as the input for the H-bridge DC-AC inverter. The EMS output filter included a capacitor C_{fil} of 13.2 μF, and an inductor L_{fil} of 1.16 mH. The two loads were purely resistive. The critical load resistance was variable and consisted of three parallel resistors measuring 1200 Ω, 600 Ω, and 300 Ω, which could be switched in and out of the circuit. The non-critical load resistance was 400 Ω. The threshold for turning on EMS current $I_{ems\text{-}on}$ was set at 0.32 A, and the threshold for turning off EMS current $I_{ems\text{-}off}$ was set at 0.39 A. The threshold to shed non-critical loads I_{max} while connected to the grid was set at 0.78 A and while islanded was set at 0.44 A. The threshold to restore non-critical loads I_{maxoff} while connected to the grid was set at 0.32 A and while islanded was set at 0.16 A.

2. Peak Power Control with the Main Grid Connected

Peak power control was achieved in the lab by monitoring the rms current in the load. With the microgrid connected to the main power source, scenario one of Figure 15 was implemented in the laboratory. In this scenario the H-bridge inverter in the EMS was controlled as a current source. As discussed in Chapter III.C, the EMS regulated the DC-AC inverter to provide an EMS current I_{ems} equal to half of the load current. This resulted in reducing the peak power drawn from the main power source without load shedding. This scenario is demonstrated with the experimental measurements displayed in Figure 26. The waveforms reveal that when the critical load increases $I_{critical}$, the total load current I_{load} is increased and the EMS provides supplemental current equal to half of the load current. This occurs because the total load current I_{load} exceeds $I_{ems\text{-}on}$. The critical load resistance was decreased from 1200 Ω to 400 Ω. A delay between the load increase and the EMS current turning on can be seen in Figure 26. This delay was primarily due to the rms current computation algorithm. The top waveform in Figure 26 V_{cfil} is the AC bus voltage across the capacitor C_{fil} in Figure 17.

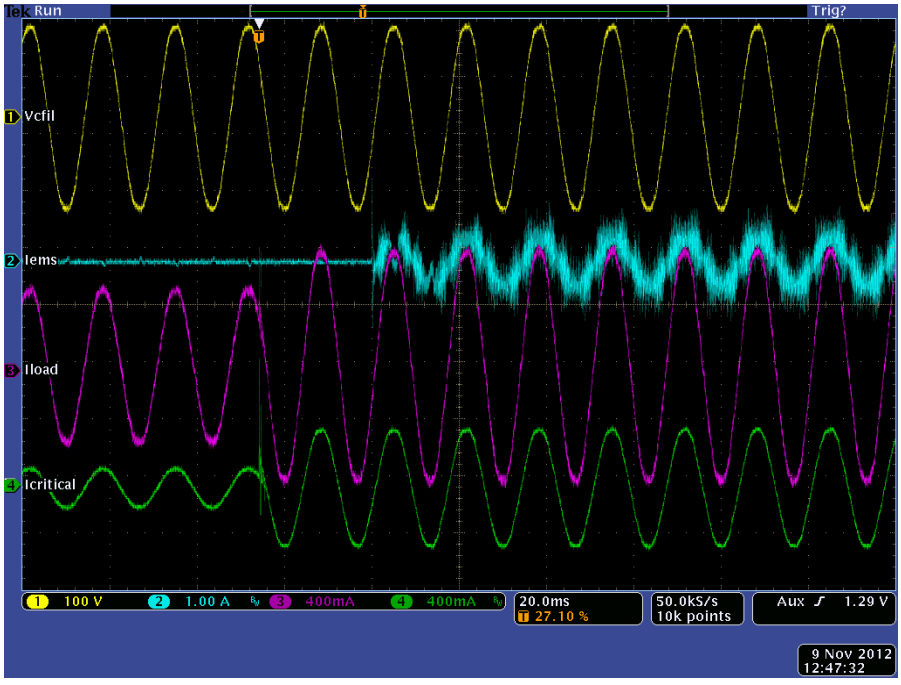

Figure 26. Experimental measurements demonstrating peak current control with the EMS providing some of the load current.

Scenario three of Figure 15, depicting peak power control with non-critical load shedding, was implemented in simulations and then validated in the lab. In this scenario the critical load resistance was decreased from 400 Ω to 171 Ω. The resulting load current I_{load} was greater than the load current shedding threshold I_{max}, and the non-critical load was shed. The thresholds for load shedding I_{max} and load restoration I_{maxoff} while connected to the grid were 0.78 A and 0.32 A, respectively. The simulation of the load shedding transient, illustrated in scenario three of Figure 15, using the Simulink model is shown in Figure 27. The experimental waveforms for the same scenario implemented in the laboratory set up are shown in Figure 28. The critical load current $I_{critical}$ is never interrupted as shown by the bottom waveform of Figure 28. The load current I_{load} is reduced when it exceeds the load shedding threshold I_{max}. The load current I_{load} is reduced by shedding the non-critical load. The EMS current is not interrupted during the scenario.

In both Figures 27 and 28, approximately 70 ms of delay between the critical load increase and the non-critical load shedding is seen. The delay between the two events is primarily due to the time required for the load current I_{load} rms value to update.

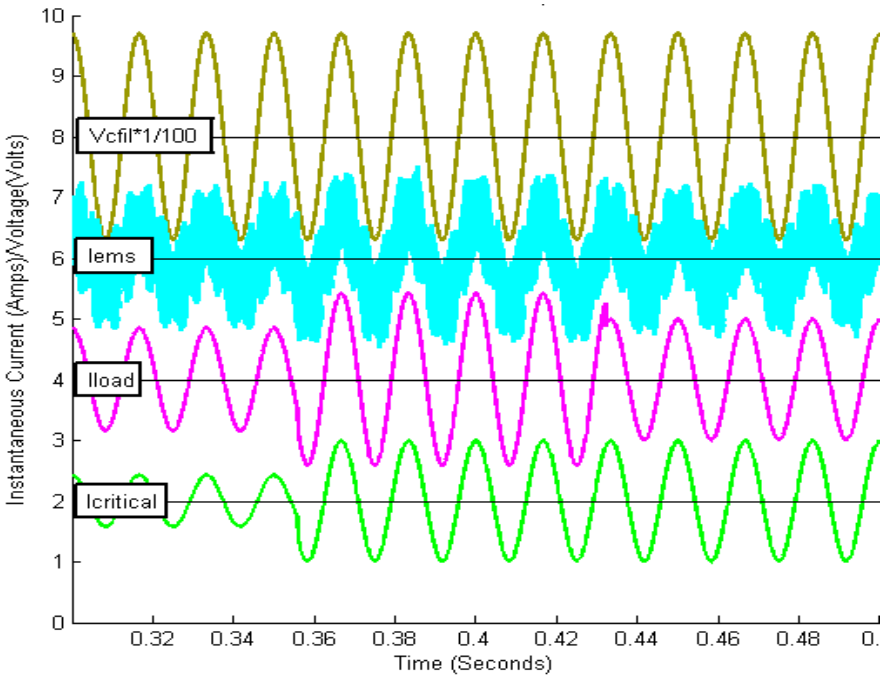

Figure 27. Simulated plots of the load shedding scenario with the main power source connected. Waveforms are offset from zero to correlate with Figure 28.

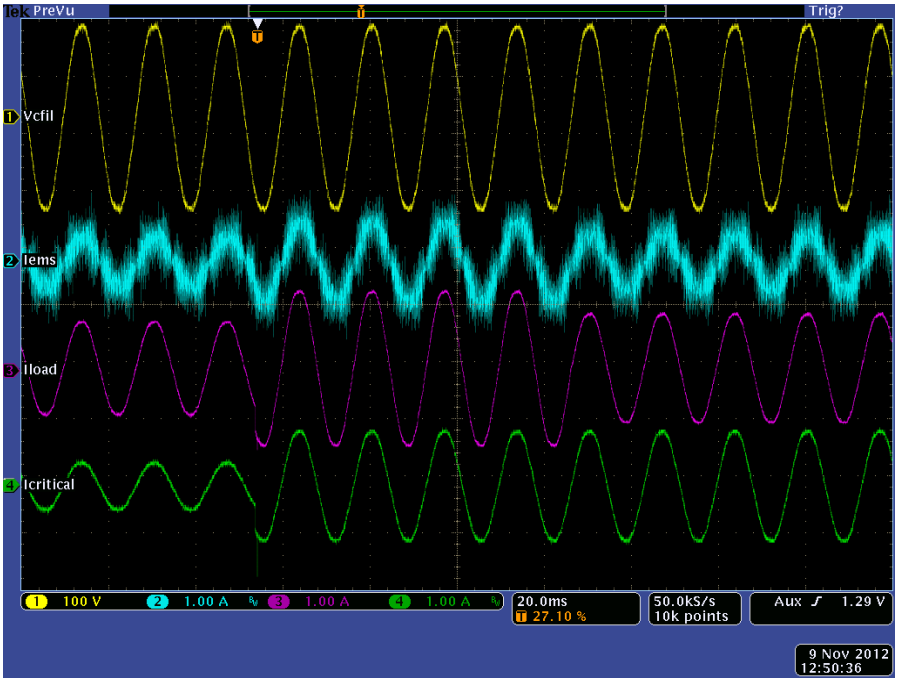

Figure 28. Experimental plots of the load shedding scenario with the main power source connected.

3. Peak Power Control in Islanding Mode

Load shedding and load restoration events while the microgrid was islanded are demonstrated in Figures 29 and 30, respectively. For these experiments the thresholds for load shedding I_{max} and load restoration I_{maxoff} were 0.44 A rms and 0.16 A rms, respectively. The critical load resistance was decreased from 1200 Ω to 400 Ω when recording the data captured in Figure 29. This caused the total load current I_{load} to increase beyond the threshold I_{max}. The EMS was the only power source providing load current, so it reacted by shedding the non-critical load. Note that the critical load is undisturbed while the non-critical load is shed.

The critical load resistance was then increased from 400 Ω to 1200 Ω to generate Figure 30. This caused the EMS to restore the non-critical load since the total load current falls below the I_{maxoff} threshold. Note that the time delay during load restoration, as seen in Figure 30, is approximately 20 ms faster than the delay seen during load shedding, Figure 29.

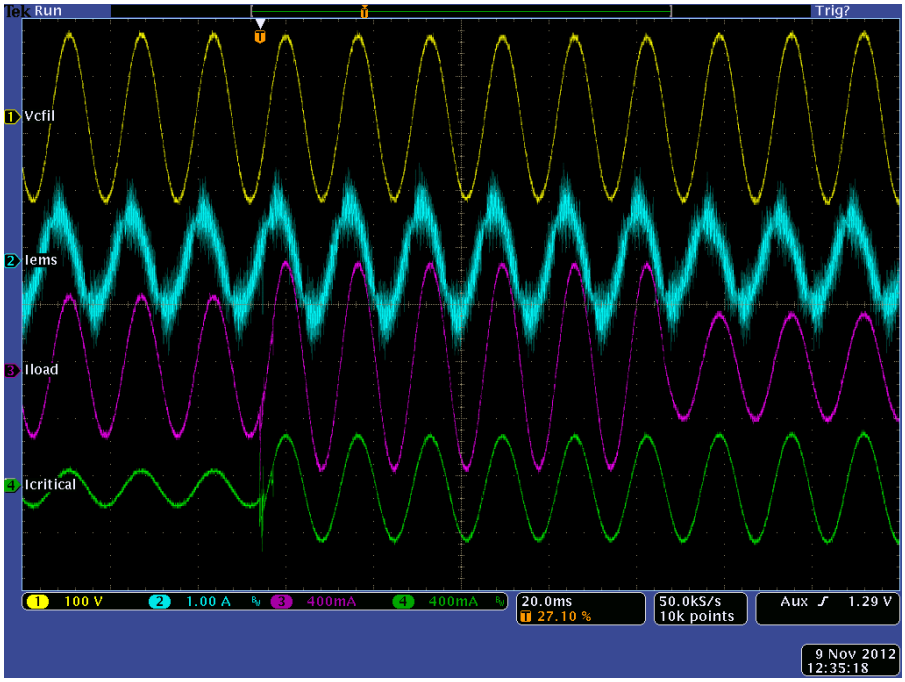

Figure 29. Experimental plots of load shedding while the microgrid is islanded.

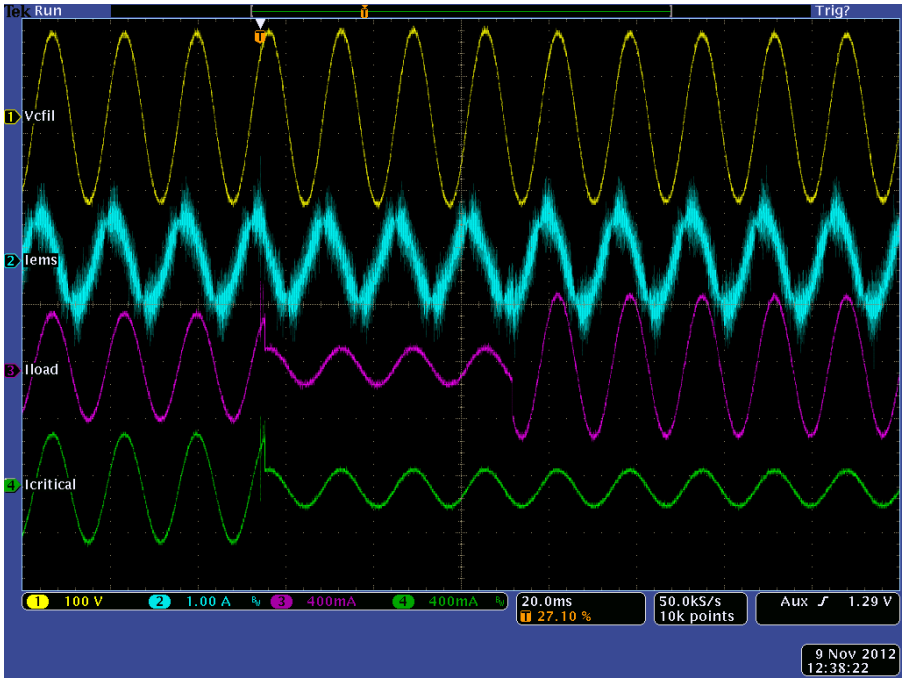

Figure 30. Experimental plots of non-critical load restoration while the microgrid is islanded.

4. EMS Powering Critical Loads when the Main Power Source Fails

In order to provide power to critical loads when the main power source fails, the EMS detects commercial electricity grid failure. This is scenario two illustrated in Figure 15. The voltage and current waveforms measured when the commercial electricity grid is disconnected, and the EMS begins operating as a voltage source are shown in Figure 31. Before the commercial electricity grid power failure, the non-critical and critical loads were on, both with a resistance of 400 Ω. The commercial electricity grid failure was initiated with a manual breaker. After the commercial electricity grid fails, the EMS provides power to the microgrid. The non-critical load is shed and only the critical load is serviced. It should be noted that the response time of the EMS was slow and resulted in an interruption in power of approximately 20 ms.

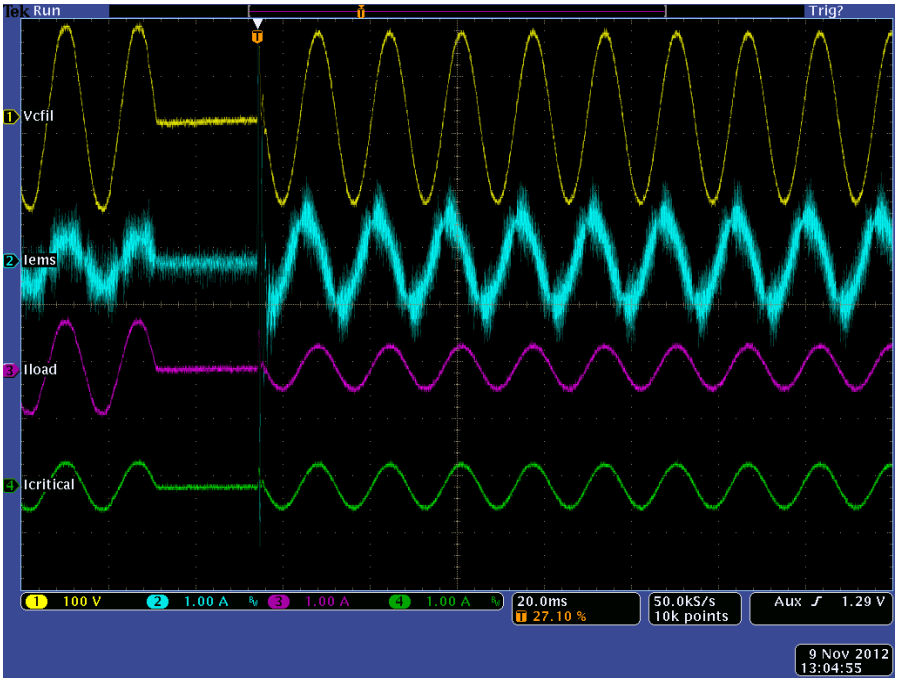

Figure 31. Experimental plots of the microgrid islanding and load shedding.

G. CHAPTER SUMMARY

In this chapter, the physics based model of the EMS and microgrid were presented. The hardware used to implement the EMS was discussed. Three scenarios were presented to show the functionality of the EMS and to verify the physics based model as a tool for additional research. In the next chapter, the simulation results of the validated EMS model managing a more complex microgrid are discussed.

IV. EMS CONTROLLED MICROGRID MODEL SIMULATIONS

A. INTRODUCTION

The Simulink model presented in Chapter III has been experimentally validated. It is now a tool that can be used to design more complex systems and to predict their behavior. In particular, scenarios with more than two loads, which can be non-resistive, can be simulated to demonstrate more aspects of the EMS functionality.

B. LOAD MODELING

1. Single-Phase Induction Machine

An unsymmetrical single-phase induction machine was used to simulate a motor load in a household. For the following simulations, a single phase, 4-pole, ¼-hp, 110 V, 60 Hz capacitor-start, capacitor-run machine is used. This was chosen because machine variables and a model of them were readily available from [26] and [27], respectively. It was also chosen because of the likelihood of this type of load in a single family home or DoD facility.

2. Single-Phase Diode Rectifier

A single-phase diode rectifier was used to simulate a load such as a PC power supply or other similar electronic power supplies. The complexity of this model was limited to the diode rectifier and a resistive load. This was chosen because a model was readily available from [28] and because of the likelihood of this type of load in a single family home or DoD facility.

C. EMS MANAGING MORE COMPLEX LOADS

1. Setup

The circuit in Figure 32 was modeled and simulated using Simulink. The circuit consists of four loads, two critical and two non-critical. The two critical loads are a single-phase diode rectifier and a resistor. The two non-critical loads are a single-phase induction machine and a resistor. The EMS prioritizes the non-critical motor load above

the non-critical resistive load. The load shedding threshold I_{max} is set to 43 A rms. The shed load restoration threshold I_{maxoff} is equal to the load shedding threshold minus the peak non-critical load current, which is 16 A rms. The EMS current threshold $I_{ems\text{-}on}$ is half of the load shedding threshold or 21.5 A rms. The threshold to secure EMS current $I_{ems\text{-}off}$ is 90% of $I_{ems\text{-}on}$ or 19.35 A rms. The simulation is 4.0 s long. Both the resistive loads turn on at 0.11 s. The diode rectifier load turns on at 0.4 s and off at 3.0 s. The motor load turns on at 0.6 s and remains on for the rest of the simulation.

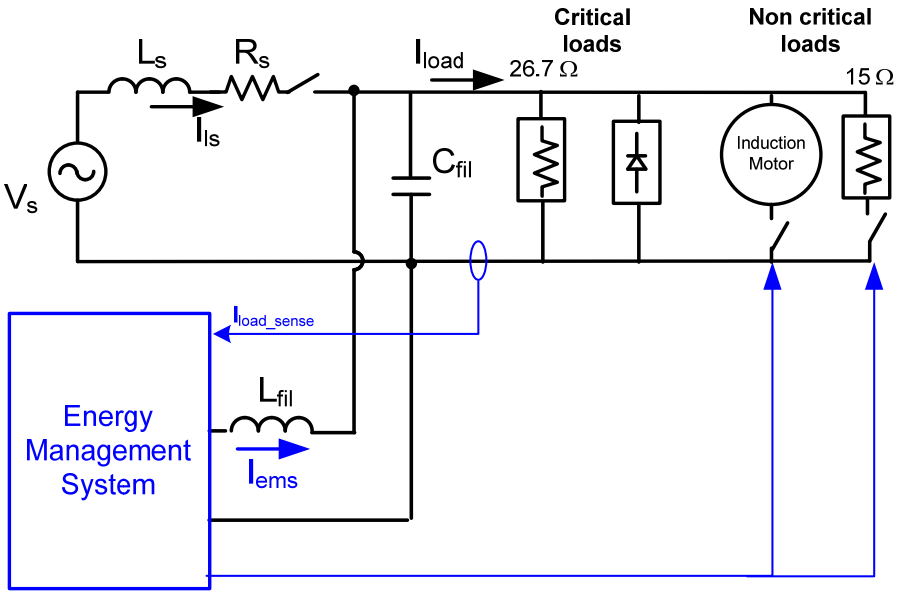

Figure 32. Circuit schematic of the simulated scenario.

Three simulations were performed to show the behavior of the microgrid with and without the EMS. Simulation results are shown in Figure 33, Figure 36, and Figure 37 for the following modes of operation, respectively:

i. The EMS is fully operational. The EMS provides half of the load current I_{load} when the load current I_{load} is larger than the EMS current threshold $I_{ems\text{-}on}$. A non-critical load is shed when the load current I_{load} exceeds the load shedding threshold I_{max}.

ii. The EMS is operational without load shedding enabled. The EMS provides half of the load current I_{load} when the load current I_{load} is larger than the EMS current threshold $I_{ems\text{-}on}$ but does not control the non-critical loads.

iii. The EMS is disabled.

2. EMS Fully Operational

The rms values of the source current I_{ls}, load current I_{load}, and EMS current I_{ems}, are plotted together with the load current thresholds in Figure 33. The $I_{ems\text{-}off}$ threshold is not shown in Figure 33. In the simulations plots of Figure 33, the following events are labeled:

1) The EMS current I_{ems} turns on because the load current I_{load} crosses the EMS current threshold $I_{ems\text{-}on}$.

2) The non-critical resistive load is shed because the load current I_{load} becomes larger than the load shedding threshold I_{max}.

3) The single-phase induction machine transitions from capacitor-start to capacitor-run, which reduces the load current I_{load} but has no effect on EMS operation.

4) The diode rectifier is turned off and the load current I_{load} goes below the shed load restoration threshold I_{maxoff}.

5) The non-critical resistive load previously shed is now turned back on automatically.

The EMS was fully operational for the simulation illustrated in Figure 33. It can be seen in Figure 33 that when the load current I_{load} exceeds the EMS current threshold $I_{ems\text{-}on}$, the EMS supplies current I_{ems} to reduce the main power source current I_{ls}. The motor start at 0.6 s increases the load current I_{load} above the load shedding threshold I_{max}. The EMS sheds the non-critical resistive load to reduce the main power source current I_{ls} as seen in Figure 34. This reduces the load current I_{load} below the load shedding threshold I_{max} during the motors start up cycle. The circuit reaches a steady-state condition just

before 3.0 s, and then the diode rectifier turns off at 3.0 s. This causes the load current I_{load} to drop below the shed load restoration threshold I_{maxoff}, and the non-critical resistive load is restored.

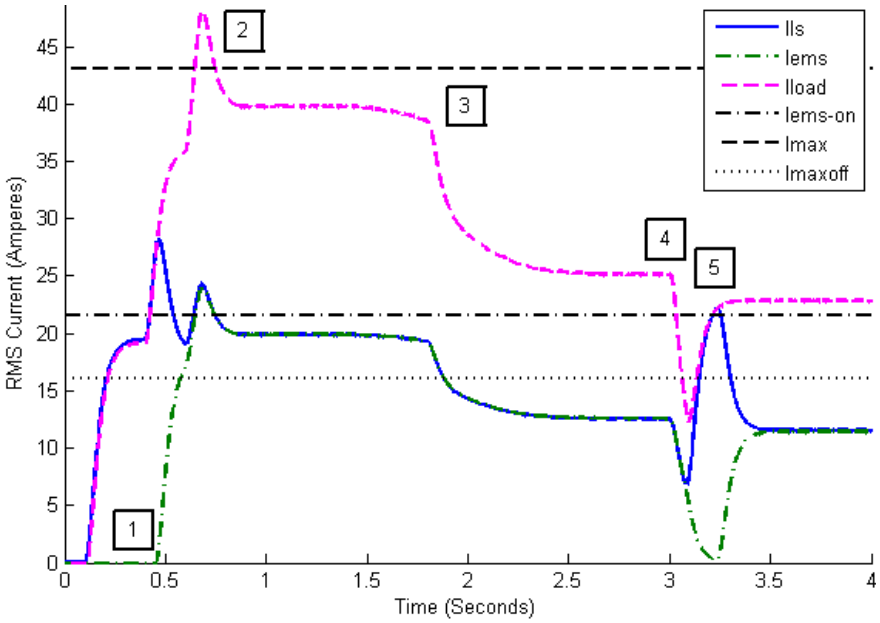

Figure 33. Simulation plots with the EMS fully operational.

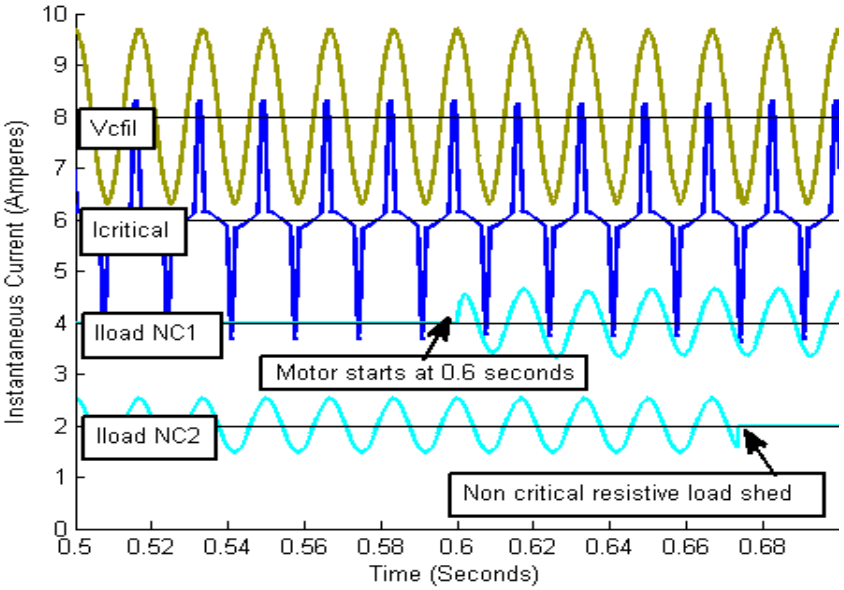

Figure 34. Simulated waveforms showing a lower priority non-critical load being shed. V_{cfil} is 1/100th of actual value. Currents are 1/40th of actual values. Each waveform is offset from zero by multiples of 2.

The shed load restoration threshold I_{maxoff} is the load shedding threshold I_{max} minus the peak non-critical load current. This threshold was chosen to prevent non-critical load oscillations when shedding loads. A non-critical load restoration threshold above this value could result in non-critical load oscillations as illustrated in Figure 35.

In the simulation plots of Figure 35, the following events are labeled:

1) The EMS current I_{ems} turns on because the load current I_{load} crosses the EMS current threshold $I_{ems\text{-}on}$.

2) The non-critical resistive load is shed because the load current I_{load} becomes larger than the load shedding threshold I_{max}.

3) The non-critical resistive load is restored because the load current I_{load} drops below the shed load restoration threshold I_{maxoff}.

4) The non-critical resistive load is turned on and off by the EMS because the shed load restoration threshold I_{maxoff} is too high.

5) The single-phase induction machine transitions from capacitor-start to capacitor-run, and the load current I_{load} drops below and stays below the load shedding threshold I_{max}.

6) The diode rectifier is turned off but does not affect EMS operation.

Figure 35 was generated using an I_{maxoff} threshold of 40 A rms. The I_{maxoff} threshold of 40 A rms resulted in load oscillations upon shedding of any of the non-critical loads. The disadvantage of a threshold to restore shed loads that ensures no load oscillations is a system that does not maximize the power available to it. Specifically, non-critical loads whose operation would not result in the load current exceeding I_{max} are still prevented from operating unless operator action is taken. This is evident in Figure 33 and Figure 35. The case where the shed non-critical load could have been restored without exceeding the I_{max} threshold is illustrated in Figure 33. At approximately 2.0 s, the motor transitions from capacitor-start to capacitor-run, and a drop in the load current is observed. After this event, the shed non-critical resistive load could have been restored without exceeding I_{max}. The expected load current I_{load} if the shed non-critical resistive

load were restored following the motors transition from capacitor-start to capacitor-run is seen in Figure 35 between 2.5 and 3.0 s. A more capable algorithm is needed to overcome this drawback, but for the hardware implemented in the lab and the Simulink model, it was overcome with operator action to restore shed non-critical loads. This was implemented with a disable/clear load shedding user input for the EMS.

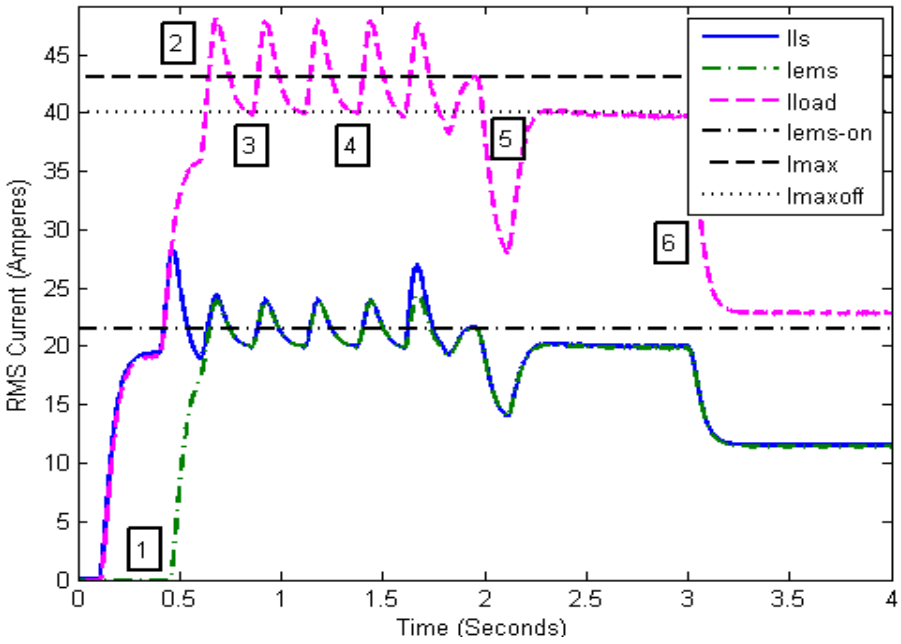

Figure 35. Simulation plots with the EMS fully operational, but with an I_{maxoff} value set high enough to cause load oscillations.

3. EMS with Load Shedding Disabled

In the simulations plots of Figure 36, the following events are labeled:

1) The EMS current I_{ems} turns on because the load current I_{load} crosses the EMS current threshold $I_{ems\text{-}on}$.

2) The single-phase induction machine turns on but no loads are shed and the load current I_{load} exceeds the load shedding threshold I_{max}.

3) The single-phase induction machine transitions from capacitor-start to capacitor-run and causes the load current I_{load} to drop below the load shedding threshold I_{max}.

4) The diode rectifier is turned off but does not affect EMS operation.

The mode of operation with the EMS enabled but without the load shedding capability is illustrated in Figure 36. The disadvantage of operating without load shedding is that the system may exceed the maximum load current threshold, which could result in loss of power to the entire system instead of just the non-critical loads. The advantage of operating without load shedding is a circuit that always responds to load demand as long as circuit breaker ratings are not exceeded. Comparing Figure 33 and Figure 36, we see that the load current peak is measurably reduced by the load shedding feature of the EMS. As a consequence, the peak of the current drawn from the main power source I_{ls} is reduced.

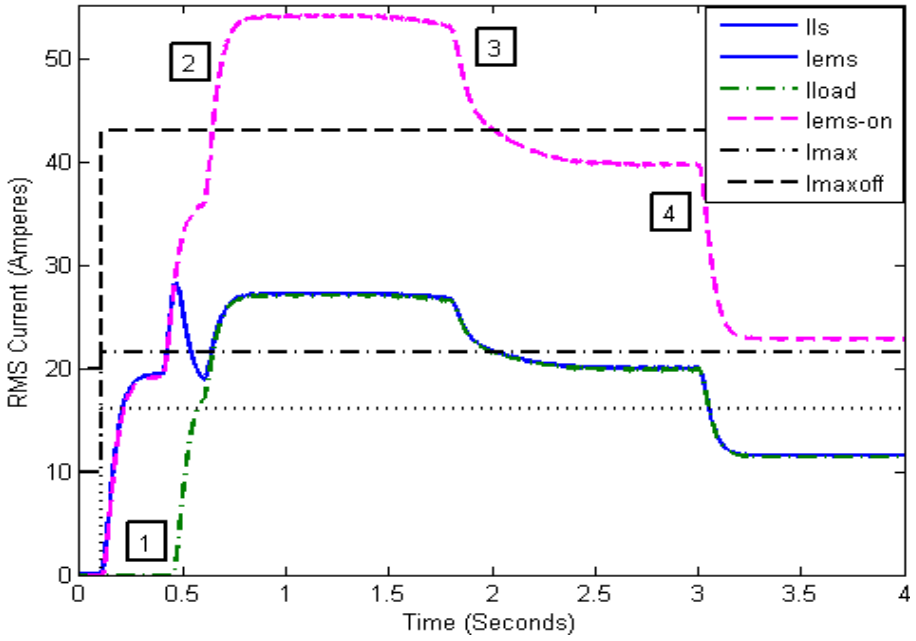

Figure 36. Simulation plots with the EMS load shedding disabled.

4. EMS Disabled

The results of the simulation with the EMS disabled are shown in Figure 37. In this case the source must support all the loads at any time. The plots clearly show that I_{load} is equal to I_{ls}. The disadvantage of such a system is the peak power demand it places

on the main power source. It requires a main power source that is sized to support the peak power demand but typically operates at a lower power demand that is less efficient.

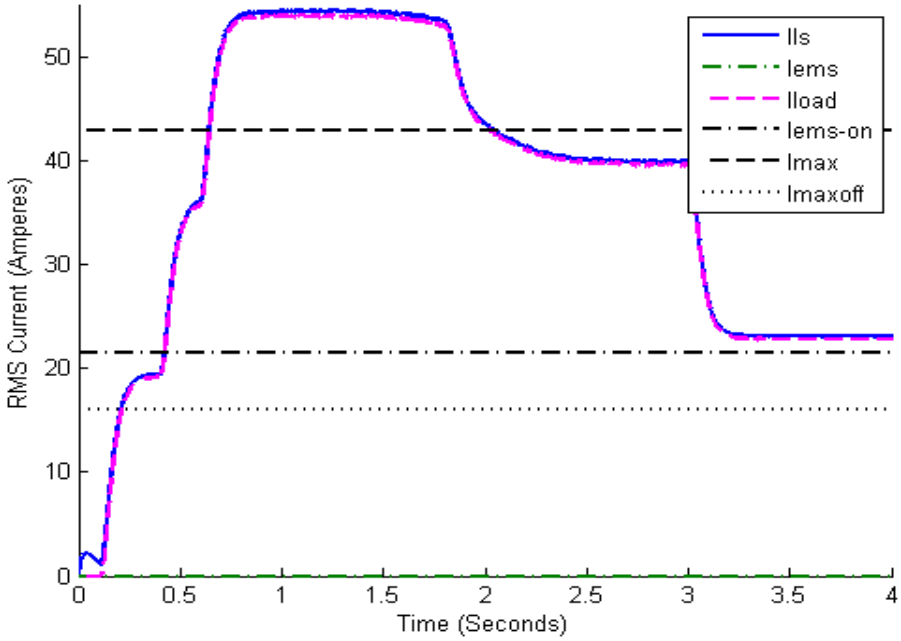

Figure 37. Simulation current plots with the EMS disabled.

D. CHAPTER SUMMARY

In this chapter, the simulation results of the validated EMS model managing a more complex microgrid were discussed. The simulation was run with the EMS fully operational, the EMS without load shedding, and the EMS disabled. Advantages and disadvantages of each mode of EMS operation were addressed.

V. CONCLUSIONS AND FUTURE RESEARCH

A. CONCLUSIONS

Problems associated with DoD facilities related to energy security and cost were presented in this thesis. One of many solutions that DoD facilities could benefit from incorporating were presented. Specifically, the incorporation of electrical microgrids and DR within the present electrical distribution of DoD facilities were focused on.

The power demand of a single family home was analyzed. The impact of peak power demand on the commercial electricity grid was emphasized. The difference between the average power demanded and the peak power demanded was discussed. A method of peak power control that would result in improved energy security and reduced energy cost was introduced.

Next, the functionality of a power electronics based EMS operating in a microgrid was presented. A physics based model was developed, experimentally validated and then used to study the functionality of the EMS. Operation of a microgrid with and without the EMS was simulated and compared. The comparison focused on the benefits and drawbacks of the EMS ability to provide supplemental current and perform load shedding. Specifically, the peak power demand on the main power source was reduced to below an established threshold, but the operation of non-critical loads was not maximized. The benefit of an EMS capable of islanding a microgrid is improved energy security.

Several function details were identified that can affect the EMS performance. The dependence of the EMS on the response time of the rms calculation was discussed. The setting of thresholds to avoid load oscillations was addressed. Lastly, an interruption in power when islanding was identified.

B. FUTURE RESEARCH

An EMS can significantly improve power reliability, availability, efficiency and quality and these advantages should be explored in future research.

The ability to restore non-critical loads in larger microgrid circuits needs to be pursued in future research if load shedding is to become a viable option to reduce peak power demand. With the logic presented in this thesis, it is reasonable to assume that load shedding would perform no differently than a manual circuit breaker if more non-critical loads were incorporated into the microgrid. The restoration of non-critical loads following a transient without user intervention is a major benefit of load shedding.

The EMS did not allow bi-directional power flow between the microgrid and the energy storage in this thesis. Future research should be done on the benefits of bi-directional power flow to reduce peak power demand and increase low power demand. It is presumed that the overall benefit would be a more constant power demand seen by the main power source, which could increase the efficiency of the main power source.

Future research should be done to determine the impact on cost savings of prioritizing energy security over cost savings. No logic was incorporated to manage the battery power level and to prevent it reaching levels that would risk energy security before cost savings. More specifically, the battery was permitted to discharge indefinitely. Additionally, the battery capacity and size needed to make the EMS a viable option for large buildings or sites needs to be researched to determine the adequacy of an EMS for such an application.

Future research into other methods of determining an rms value would benefit the response time of the system. The rms calculation used to make logic decisions delayed the required action. The amount of delay seen may be acceptable for some applications but for many a quicker response time is required.

APPENDIX. MATLAB M-FILES

A. HARDWARE LOAD SHEDDING FUNCTION FILE

```
%Nathan Peck, Thesis: Peak Power Control with an EMS
%31 October 2012, EMS Load Shedding Function for Hardware
%This function implements Load Shedding for the EMS.
function [ShedLoad2,Imax]=fcn1(Load2_on,source_on,Iload,disable_clear)


%******Load constants that the EMS depends on to make decisions******
if source_on;
%The load shedding rms current threshold, 0.78A rms, when grid
connected.
    Imax=xfix({xlUnsigned,12,9},0.78);
%The load restoration rms current threshold, 0.32A rms, when grid
connected.
    Imaxoff=xfix({xlUnsigned,12,9},0.32);
else
%The load shedding rms current threshold, 0.44A rms, when islanded.
    Imax=xfix({xlUnsigned,12,9},0.44);
%The load restoration rms current threshold, 0.16A rms, when islanded.
    Imaxoff=xfix({xlUnsigned,12,9},0.16);
end

%******************Persistent Variables*****************************
%Persistent variables are saved locally and thus still exist when the
%hardware steps out of this function and then back into this function
%on the next time step.

%ShedLoadXin represents the shed or don't shed status of loads. shed=1,
%don't shed=0
persistent ShedLoad2in, ShedLoad2in = xl_state(0, {xlBoolean});

%Boolean variables for easy assignments of a one or zero value.
one=xfix({xlBoolean},1);
zero=xfix({xlBoolean},0);

%******************Load Shedding Decision*****************************
%A boolean 1 disables/clears any load shedding.
if disable_clear;
    ShedLoad2in=zero;
%If more than one non-critical loads were supplied then based off a
different persistent variable clear the correct one.
else
    if Iload>Imax;
            if Load2_on;
                ShedLoad2in=one;    %Shed the non-critical load
%If more than one non-critical loads were supplied then the lower the
load number the higher the priority. The logic decisions would continue
as seen below.
%             elseif Load1;
```

```
%                 ShedLoad1in=zero;
            end
    elseif Iload<Imaxoff;
        ShedLoad2in=zero;     %Restore the non-critical load
    end
end
```

B. MATLAB SIMULINK MODEL M-FILES

1. Initial Condition M-File for Resistive Load Case

```
%Nathan Peck, Thesis: Peak Power Control with an EMS
%5 February 2013, Model Simulation Initial Conditions
%Load model characteristics taken from Prof. Oriti and
%Prof. Julian simulation model initial condition file
%EMS_ic_v4 dated 23 April 2012 or as otherwise
%annotated in this file.

%Time step and simulation length
tstep=1e-6;
tstop=1;
split=10;
%Make split > tstop to run the simulation with EMS
%only, =1 to run first half with and second half
%without EMS, and =0 to run without EMS.

%Five Hz LPF used twice in series to calculate RMS
%values for current/voltage
wc=2*pi*5;

%----------------------EMS Parameters----------------------
%Load operating times
Load1Start=0.11;
Load1Stop=tstop;
Load2Start=0.11;
Load2Stop=tstop;
%Increase Load transient starts at 0.356seconds
Load3Start=0.356;
Load3Stop=tstop;
Load4Start=0.11;
Load4Stop=tstop;

%Lose the source voltage start time
LoseVs=tstop;

%----------------------Source Parameters-----------------------
%-----Source Voltage-----
%Peak value used in Simulink for source model
V_phase = 120*sqrt(2);

%-----generator 1------
Ls1=4e-6;
Cfil1=13.2e-6;
%Lfil in lab=1.16mH
```

```
Rs1=0.01;

%--------------------Load Parameters---------------------------
%-----Resistors-----
%I=0.1A rms with V=120V rms
Rload_C1=1200;
%I=0.2A rms with V=120V rms
Rload_C2=600;
%I=0.4A rms with V=120V rms
Rload_C3=300;
%I=0.3A rms with V=120V rms or 1200//600
Rload_NC1=400;

%---Single Phase Capacitor Start Capacitor Run Motor Load---
%Parameters from Krause, Analysis of Electrical Machinery
%and Drive Systems
%omega = 2*pi*60;%Modify this variable to change reference frame
omega_b = 2*pi*60;
omega_in = 2*pi*60;
twopiby3 = 2*pi/3;
wbby2H = omega_b/2/0.5;
poles = 4;
polesby2J = poles/2/.0146;

%Parameters from page 384 of Krause
capacitor=1/14.5/omega_b;
Zc_run=172;
capacitor_run=1/Zc_run/omega_b;
rC=3;
rC_run=9;
NS_by_Ns=1.18;
Xms =66.8;
XmS =92.9;

rs=2.02;
rS=7.14;
rr = 4.12;
rR = 5.74;
Xls =2.79;
XlS=3.22;
Xlr = 2.12;
XlR=2.95;

% Eqs 10.4–39 to 10.4–42 of Krause
coeff_mat=[Xls+Xms 0 Xms 0; 0 XlS+XmS 0 XmS; Xms 0 Xlr+Xms 0; 0 XmS 0
XlR+XmS];
inv_coeff_mat=inv(coeff_mat);

%-----Diode Rectifier Load-----
%EC3150 Software lab#4 - Diode Rectifier - Dr. Giovanna Oriti
%initial conditions file for model ec3150_software_lab4.mdl
ampl=29*sqrt(2);
fund=60;
ws=2*pi*fund;
```

```
Ls=200e-6;  %original
%Ls=2e-4;  %reduced source inductance
Rs=5e-3;
Rload=10;
Cdc=1100e-6;

%-----H-Bridge Model-----
%EC3150 Software lab#5 - H-bridge inverter - Dr. Giovanna Oriti
%initial condition file for model ec3150_software_lab5.mdl

Kp_v=0.06;
Ki_v=5000;
sw_freq=15000;
Vdc=200;
%A 1 is Bipolar PWM. A 0 is Unipolar PWM. Unipolar PWM used.
PWM_mode=0;
Lfil=1.16e-3;

%Parameters used in lab but not for EMS model
%Vdc=130; original in lab
%vo_ref=120*sqrt(2)*2/pi;
%turns=28/115;
%Rload=2000;
%Lin=3.22e-3;
%tstep = 1e-6;
```

2. Load Shedding and EMS Current Function M-File for Resistive Load Case

```
function [ShedLoad2,EMSvoltageon,Imax,EMScurrenton]...
    = EMS(Load2_on,source_on,disable_clear,Iload)
%This function implements the EMS

%*********************Persistent Variables*****************
%Persistent variables are saved locally and thus still
%exist when the simulation steps out of this function
%and then back into this function on the next time step.

persistent ShedLoad2in;
if isempty(ShedLoad2in);
    ShedLoad2in=0;
end
persistent EMScurrent;
if isempty(EMScurrent);
    EMScurrent=0;
end
persistent EMSvoltage;
if isempty(EMSvoltage);
    EMSvoltage=0;
end

%Determine Imax based off the source current being available
if source_on>0.6;
    Imax=0.78;
```

```
    Imaxoff=0.32;
    EMSvoltage=0;
    %Determine if supplemental EMS current should be provided or not.
    if Iload>0.39;  %Iems-on=0.39
        EMScurrent=1;
    elseif Iload<0.32   %Iems-off=0.32
        EMScurrent=0;
    end
%If the source is not availabe use these thresholds
else
    Imax=0.44;
    Imaxoff=0.16;
    EMSvoltage=1;
    EMScurrent=0;
end

%Determine if Non-Critical Loads should be shed or restored.
if disable_clear>0.6;
    ShedLoad2in=0;
else
    if Iload>Imax;
        if Load2_on>0.6;
            ShedLoad2in=1;
        end
    elseif Iload<Imaxoff;
        ShedLoad2in=0;
    end
end

%***Assign the output values to the persistent variable values***
%A 0 allows the load to turn ON
ShedLoad2=ShedLoad2in;
%A 1 turns on the EMS current
EMScurrenton=EMScurrent;
%A 1 disconnects the source and turns on EMS voltage
EMSvoltageon=EMSvoltage;
```

3. Initial Condition M-File for Complex Load Case

```
%Nathan Peck, Thesis: Peak Power Control with an EMS
%5 February 2013, Model Simulation Initial Conditions
%Load model characteristics taken from Prof. Oriti and
%Prof. Julian simulation model initial condition file
%EMS_ic_v4 dated 23 April 2012 or as otherwise
%annotated in this file.

%Time step and simulation length
tstep=1e-6;
tstop=4;
split=10;
%Make split > tstop to run the simulation with EMS
%only, =1 to run first half with and second half
%without EMS, and =0 to run without EMS.
```

```
%Five Hz LPF used twice in series to calculate RMS
%values for current/voltage
wc=2*pi*5;

%--------------------Load operating times-------------------

%Critical Resistive Load
Load1Start=0.11;
Load1Stop=tstop;
Load2Start=0.11;
Load2Stop=tstop;
Load3Start=0.11;
Load3Stop=tstop;
%Induction Machine Load
Load4Start=0.6;
Load4Stop=tstop;
%Non Critical Resistive Load
Load5Start=0.11;
Load5Stop=tstop;
%Rectifier Load
Load6Start=0.4;
Load6Stop=3;

%Lose the source voltage
LoseVs=tstop;
%Set to 0 to Disable/Clear Load Shedding
%Set to any value >tstop to enable Load Shedding
Disable_Clear=10;

%----------------------Source Parameters------------------------
%-----Source Voltage-----
%Peak value used in Simulink for source model
V_phase = 120*sqrt(2);

%-----generator 1------
Ls1=4e-6;
Cfil1=13.2e-6;
%Lfil in lab=1.16mH
Rs1=0.01;

%-----------------------Load Parameters------------------------
%-----Resistors-----
%Critical Lighting
%I=1.5A rms with V=120V rms, represents 3 Lightbulbs in parallel
Rload_C1=80;
%I=1.5A rms with V=120V rms, represents 3 Lightbulbs in parallel
Rload_C2=80;
%I=1.5A rms with V=120V rms, represents 3 Lightbulbs in parallel
Rload_C3=80;
%Non-Critical Lighting
%I=8A rms with V=120V rms, represents 16 Lightbulbs in parallel
Rload_NC1=8;

%---Single Phase Capacitor Start Capacitor Run Motor Load---
```

```
%Parameters from Krause, Analysis of Electrical Machinery
%and Drive Systems
%omega = 2*pi*60;%Modify this variable to change reference frame
omega_b = 2*pi*60;
omega_in = 2*pi*60;
twopiby3 = 2*pi/3;
wbby2H = omega_b/2/0.5;
poles = 4;
polesby2J = poles/2/.0146;

%Parameters from page 384 of Krause
capacitor=1/14.5/omega_b;
Zc_run=172;
capacitor_run=1/Zc_run/omega_b;
rC=3;
rC_run=9;
NS_by_Ns=1.18;
Xms =66.8;
XmS =92.9;

rs=2.02;
rS=7.14;
rr = 4.12;
rR = 5.74;
Xls =2.79;
XlS=3.22;
Xlr = 2.12;
XlR=2.95;

% Eqs 10.4–39 to 10.4–42 of Krause
coeff_mat=[Xls+Xms 0 Xms 0; 0 XlS+XmS 0 XmS; Xms 0 Xlr+Xms 0; 0 XmS 0
XlR+XmS];
inv_coeff_mat=inv(coeff_mat);

%-----Diode Rectifier Load-----
%EC3150 Software lab#4 - Diode Rectifier - Dr. Giovanna Oriti
%initial conditions file for model ec3150_software_lab4.mdl
ampl=29*sqrt(2);
fund=60;
ws=2*pi*fund;
Ls=200e-6;  %original
%Ls=2e-4;  %reduced source inductance
Rs=5e-3;
Rload=10;
Cdc=1100e-6;

%-----H-Bridge Model-----
%EC3150 Software lab#5 - H-bridge inverter - Dr. Giovanna Oriti
%initial condition file for model ec3150_software_lab5.mdl

Kp_v=0.06;
Ki_v=5000;
sw_freq=15000;
Vdc=200;
```

```
%A 1 is Bipolar PWM. A 0 is Unipolar PWM. Unipolar PWM used.
PWM_mode=0;
Lfil=1.16e-3;

%Parameters used in lab but not for EMS model
%Vdc=130; original in lab
%vo_ref=120*sqrt(2)*2/pi;
%turns=28/115;
%Rload=2000;
%Lin=3.22e-3;
%tstep = 1e-6;
```

4. Load Shedding and EMS Current Function M-File for Complex Load Case

```
function [ShedLoad1,ShedLoad2,EMSvoltageon,Imax,EMScurrenton]...
    = EMS(Load1_on,Load2_on,source_on,disable_clear,Iload)
%This function implements the EMS

%******************Persistent Variables**********************
%Persistent variables are saved locally and thus still exist
%when the simulation steps out of this function and then back
%into this function on the next time step.
%timerup maintains 0.15 seconds between shedding NC loads
timerup=300000;
persistent ShedLoad1in;
if isempty(ShedLoad1in);
    ShedLoad1in=0;
end
persistent ShedLoad2in;
if isempty(ShedLoad2in);
    ShedLoad2in=0;
end
persistent timer;
if isempty(timer);
    timer=timerup;
end
persistent EMScurrent;
if isempty(EMScurrent);
    EMScurrent=0;
end
persistent EMSvoltage;
if isempty(EMSvoltage);
    EMSvoltage=0;
end

%Determine Imax based off the source current being available
if source_on>0.6;
    Imax=43;
    Imaxoff=Imax-27;    %Restore when Iload<max(Iload_NC)
    EMSvoltage=0;
    %Determine if supplemental EMS current should be provided or not.
    if Iload>Imax/2;
        EMScurrent=1;
```

```
    elseif Iload<0.9*Imax/2;
        EMScurrent=0;
    end
else
    Imax=20;
    Imaxoff=4.5;
    EMSvoltage=1;
    EMScurrent=0;
end

%Determine if Non-Critical Loads should be shed or restored.
if disable_clear>0.6;
    ShedLoad2in=0;
    ShedLoad1in=0;
else
%The timer allows 0.1 seconds for power to decrease below Imax
    if Iload>Imax && timer>timerup;
        if Load2_on>0.6;
            ShedLoad2in=1;
            timer=0;
        elseif Load1_on>0.6;
            ShedLoad1in=1;
            timer=0;
        end
    elseif Iload<Imaxoff && timer>timerup;
        ShedLoad1in=0;
        ShedLoad2in=0;
    else
        timer=timer+1;

    end
end
%***Assign the output values to the persistent variable values***
%A 0 allows the load to turn ON
ShedLoad1=ShedLoad1in;
ShedLoad2=ShedLoad2in;
%A 1 turns on the EMS current
EMScurrenton=EMScurrent;
%A 1 disconnects the source and turns on EMS voltage
EMSvoltageon=EMSvoltage;
```

C. DATA PLOTTING M-FILES

1. M-File for Figure 7

```
%Nathan Peck, Thesis: Peak Power Control with an EMS
%25 October 2012, House Microgrid Usage Plotter

%These data points were taken at hourly intervals over a year.
%This file averages each hourly reading to portray the average peak
%periods throughout a year for a house located in Monterey, CA.

close all
clear all
```

```
clc

%Read the data from the xlsx file
[NUMR,TXTR,RAWR]=xlsread('House_Annual_Data','Compiled','A1:NC26');

figure(1)
time=NUMR(1:24,1);
Power=[];
n=1;
while n<25;
    Power=[Power;sum(NUMR(n,2:length(NUMR)))/length(NUMR)];
    n=n+1;
end

AvePower=sum(Power)/24*ones(24,1);
plot(time,Power,'bo-',time,AvePower,'kx-','linewidth',2)
title('Single family home: Hourly real power averaged over a year');
xlabel('time (hours)'), ylabel('Real power (kW)');
axis([0 23 0 1.5]),grid
legend('P_K_W_-_h_o_u_r_, _a_n_n_u_a_l _a_v_e_r_a_g_e','P_K_W_-
_h_o_u_r_, _a_v_e_r_a_g_e');
```

2. M-File for Figures 8 and 9

```
%Nathan Peck, Thesis: Peak Power Control with an EMS
%5 September 2012, Single Family Household Data_Plotter

%Data recorded on 9/12/2012 from 0000 to 2400.
%This file reads raw data obtained using a Power Meter(Fluke 434)
%hooked up to the distribution panel at my house. The data is
%exported from the Power Meter(Fluke 434)into an xlsx file which
%is then read below. From this data a number of plots showing
%the operating characteristics of a typical house.

%The Power Meter was in Power&Energy mode.
%Plots can include: Real Power, Reactive Power, Apparent Power,
%Voltage, Current, Power Factor and Displacement Power Factor

close all
clear all
clc

%Read the data from the xlsx file
%MATLAB drops 2 decimal places(from Excel=62.666651 to MATLAB=62.6667)
[NUMR,TXTR,RAWR]=xlsread('09122012','MATLAB','A1:K2900');

%Make the time column vectors for the 24 hours of recording.
    %The data is recorded at 30 second intervals
    %(ie 24 hrs = 24*60*2 = 2880 data points.)
timesec=NUMR(19:2898,1); %Seconds
timemin=timesec/60;     %Minutes
timehour=timesec/3600;  %Hours
```

```
%%%%%%%%%%%%%%%%%%%%%%%%%%%%%%%%%%%%%%%%%%%%%%%%%%%%%%%%%%%%%%%%%%%%%%%%
%%%
%Plot the Real/Reactive/Apparent Power recorded over the time interval
figure(1)
Rpower=NUMR(19:2898,2);    %Real Power column vector
Ipower=NUMR(19:2898,3);    %Reactive Power column vector
Apower=NUMR(19:2898,4);    %Apparent Power column vector

%Plot the Real/Reactive/Apparent Power recorded over the time interval
%together.
plot(timehour,Rpower,'b',timehour,Ipower,'g',timehour,Apower,'r','linew
idth',1);
title('Single Family Home: Power from 0000 to 2400 on 9/12/2012');
xlabel('Time (Hours)');
ylabel('Power (W/VAR/VA)');
legend('Real Power (W)','Reactive Power (VAR)','Apparent Power
(VA)','Location','NorthWest');
axis([0 max(timehour) min(Apower) max(Apower)]);

%%%%%%%%%%%%%%%%%%%%%%%%%%%%%%%%%%%%%%%%%%%%%%%%%%%%%%%%%%%%%%%%%%%%%%%%
%%%
%Plot the Total RMS Current over the time interval
figure(2)
Acurrent=NUMR(19:2898,7);    %Line A line current column vector
Bcurrent=NUMR(19:2898,8);    %Line B line current column vector

ABcurrent=Acurrent+Bcurrent;
plot(timehour,ABcurrent,'m','linewidth',2);
title('Single Family Home: Current from 0000 to 2400 on 9/12/2012');
xlabel('Time (Hours)'), ylabel('Current (Amps)');
legend('RMS Current (Amps)','Location','NorthWest');
axis([0 max(timehour) 0 max(ABcurrent)]);
```

3. M-File for Figures 10, 11 and 12

```
%Nathan Peck, Thesis: Peak Power Control with an EMS
%15 September 2012, Load_Operating_Plotter

%This file reads raw data obtained using a Power Meter (Fluke 434)
%hooked up to the distribution panel at my house or a power cable from
%the load to an outlet. The data is exported from the Power
%Meter(Fluke 434)into an xlsx file which is then read below. From this
%data a number of plots showing the operating characteristics of a
%typical household load identified below.

close all
clear all
clc

%Read the data from the xlsx file (Covers 1 hours worth of data
%recorded at 1 second data grabs (rows taken from excel file)).
%MATLAB drops 2 decimal places (from Excel=62.666651 to MATLAB=62.6667)
[NUMR,TXTR,RAWR]=xlsread('Loads','MATLAB_Dryer','A1:V3620');
```

```
%%%%%%%%%%%%%%%%%%%%%%%%%%%%%%%%%%%%%%%%%%%%%%%%%%%%%%%%%%%%%%%%%%%%%%%%%%%%
%                          DRYER

%Power & Energy Mode

%Make the time column vectors for the recording.
cp3timesec=NUMR(19:1330,15); %Seconds
cp3timemin=cp3timesec/60;     %Minutes

%Make the Real/Reactive/Apparent Power data vectors
cp3Rpower=NUMR(19:1330,16);    %Real Power column vector
cp3Ipower=NUMR(19:1330,17);    %Reactive Power column vector
cp3Apower=NUMR(19:1330,18);    %Apparent Power column vector

figure(1)
plot(cp3timemin,cp3Rpower,'b','linewidth',2);
title('Dryer: Real Power');
xlabel('Time (Minutes)'), ylabel('Real Power (Watts)');
axis([0 max(cp3timemin) min(cp3Rpower)-10 max(cp3Rpower)+10]);
figure(2)
plot(cp3timemin,cp3Ipower,'g','linewidth',2);
title('Dryer: Reactive Power');
xlabel('Time (Minutes)'), ylabel('Reactive Power (Volts-Amps
Reactive)');
axis([0 max(cp3timemin) min(cp3Ipower)-10 max(cp3Ipower)+10]);
figure(3)
plot(cp3timemin,cp3Apower,'r','linewidth',2);
title('Dryer: Apparent Power');
xlabel('Time (Minutes)'), ylabel('Apparent Power (Volt-Amps)');
axis([0 max(cp3timemin) min(cp3Apower)-10 max(cp3Apower)+10]);

%Plot the RMS line voltage and RMS current recorded.
cp3voltage=NUMR(19:1330,19);    %RMS Voltage column vector
cp3current=NUMR(19:1330,20);    %RMS Current column vector

figure(4)
plot(cp3timemin,cp3voltage,'k',…
      cp3timemin,cp3current,'m','linewidth',2);
title('Dryer: Line RMS Voltage & RMS Current');
xlabel('Time (Minutes)');
ylabel('Current (Amps)          Voltage (Volts)');
legend('Line Voltage','Line Current','Location','West');
axis([0 max(cp3timemin) 0 max(cp3voltage)+10]);
```

4. M-File for Figure 13

```
%Nathan Peck, Thesis: Peak Power Control with an EMS
%23 September 2012, Load_Operating_Plotter

%Data recorded on 9/27/2012 and 10/1/2012
%This file reads raw data obtained using a Power Meter(Fluke 434)
%hooked up to the distribution panel at my house or a power cable
%from the load to an outlet. The data is exported from the Power
```

```
%Meter(Fluke 434)into an xlsx file which is then read below.
%From this data a number of plots showing the operating
%characteristics of a typical household load identified below.

close all
clear all
clc

%Read the data from the xlsx file.
%MATLAB drops 2 decimal places(from Excel=62.666651 to MATLAB=62.6667)
[NUMR,TXTR,RAWR]=xlsread('Loads','MATLAB_Refrigerator','A1:T3620');

%%%%%%%%%%%%%%%%%%%%%%%%%%%%%%%%%%%%%%%%%%%%%%%%%%%%%%%%%%%%%%%%%%%%%%%%%%%%
%                          REFRIGERATOR

%Power & Energy Mode

%Make the time column vectors for the recording.
%The data is recorded at 1 second intervals
%(ie 1 hrs = 60*60 = 3600 data points.)
cp3timesec=NUMR(19:437,13); %Seconds
cp3timemin=cp3timesec/60;     %Minutes

%Plot the Line voltage and current recorded over the time interval
%together.
cp3voltage=NUMR(19:437,17);    %A line voltage column vector
cp3current=NUMR(19:437,18);    %B line voltage column vector

figure
plot(cp3timemin,cp3current,'m','linewidth',2);
title('Refrigerator: RMS Current');
xlabel('Time (Minutes)'), ylabel('Current (Amps)');
legend('RMS Current','Location','SouthWest');
axis([0 max(cp3timemin) 0 max(cp3current)+1]);
```

5. M-File for Figure 14

```
%Nathan Peck, Thesis: Peak Power Control with an EMS
%23 September 2012, Load_Operating_Plotter

%Data recorded on 9/23/2012
%This file reads raw data obtained using a Power Meter(Fluke 434)
%hooked up to the distribution panel at my house or a power cable
%from the load to an outlet. The data is exported from the Power
%Meter(Fluke 434)into an xlsx file which is then read below.
%From this data a number of plots showing the operating
%characteristics of a typical household load identified below.

close all
clear all
clc

%Read the data from the xlsx file.
```

```
%MATLAB drops 2 decimal places (from Excel=62.666651 to MATLAB=62.6667)
[NUMR,TXTR,RAWR]=xlsread('Loads','MATLAB_CoffeePot','A1:T3620');

%%%%%%%%%%%%%%%%%%%%%%%%%%%%%%%%%%%%%%%%%%%%%%%%%%%%%%%%%%%%%%%%%%%%%%%%%%%
%                          COFFEE POT

%Dips & Swells Mode

%Make the time column vectors for the recording.
    %The data is recorded at 1 second intervals
    %(ie 1 hrs = 60*60 = 3600 data points.)
cptimesec=NUMR(19:1906,1); %Seconds
cptimemin=cptimesec/60;     %Minutes

%Plot the RMS voltage and current over the time interval.

cpvoltage=NUMR(19:1906,2);    %Voltage column vector
cpcurrent=NUMR(19:1906,3);    %Current column vector

figure(10)
plot(cptimemin,cpcurrent,'b','linewidth',2);
title('Coffee Pot: RMS Current');
xlabel('Time (Minutes)'), ylabel('Current (Amps)');
legend('RMS Current','Location','West');
axis([0 max(cptimemin) 0 max(cpcurrent)+1]);
```

6. M-File for Figure 27

```
%Nathan Peck, Thesis: Peak Power Control with an EMS
%9 September 2012, Simulation_Plotter

%This file calls the EMS simulation and plots the
%results for comparison.

close all;
clear all;
clc

%This runs the simulation and the variables going to
%the workspace can be plotted or manipulated to show
%results.
sim EMS_Peck_Lab;

%This for loop creates a timesec column vector to plot
%the xaxis of the various plots.
timesec=ones(1,tstop/tstep+1);
for n=(1:tstop/tstep+1)
    timesec(1,n)=n*timesec(1,n);
end
timesec=tstep*timesec;

%%%%%%%%%%%%%%%%%%%%%%%%%%%%%%%%%%%%%%%%%%%%%%%%%%%%%%%%%%%%%%%%%%%%%%%%%%%
%This figure plots the Waveforms to match an O-scope
```

```
%figure***Instantaneous Values***
figure(1);
hold on
plot(timesec(300001:500000),8+Waveforms(300001:500000,1)*1/100,...
    'linewidth',2,'Color',[0.6 0.6 0])
plot(timesec(300001:500000),6+Waveforms(300001:500000,4),...
    '-c','linewidth',2)
plot(timesec(300001:500000),4+Waveforms(300001:500000,5),...
    '-m','linewidth',2)
plot(timesec(300001:500000),2+Iload_C_waveform(300001:500000),...
    '-g','linewidth',2)
plot(timesec(300001:500000),8.*ones(1,200000),'-k')
plot(timesec(300001:500000),6.*ones(1,200000),'-k')
plot(timesec(300001:500000),4.*ones(1,200000),'-k')
plot(timesec(300001:500000),2.*ones(1,200000),'-k');
axis([timesec(300001) timesec(500001) 0 10]);
legend('Vcfil*1/100','Iems','Iload','Icritical');
xlabel('Time (Seconds)'),ylabel('Instantaneous Current (Amperes)');
title('MATLAB Oscilloscope Plot');
hold off

%%%%%%%%%%%%%%%%%%%%%%%%%%%%%%%%%%%%%%%%%%%%%%%%%%%%%%%%%%%%%%%%%%%%%%%
%This figure plots Is, Iload,Iems and Imax ****RMS Values****
figure(2);
plot(timesec,RMS_Multimeter(:,2),'-b',...
    timesec,RMS_Multimeter(:,3),'-c',...
    timesec,RMS_Multimeter(:,4),...
    '-m',timesec,RMS_Multimeter(:,5),'--k','linewidth',2);
axis([0 max(timesec) 0 max(RMS_Multimeter(:,2))+1]);
legend('Ils','Iems','Iload','Imax');
xlabel('Time (Seconds)'),ylabel('RMS Current (Amperes)');
title('Source, Load, EMS and Max Current over time');
```

7. M-File for Figure 33, 34 35, and 36

```
%Nathan Peck, Thesis: Peak Power Control with an EMS
%9 September 2012, Simulation_Plotter

%This file calls the EMS simulation and plots the
%results for comparison.

close all;
clear all;
clc;

%The first row in each .mat file is the time vector for
%the simulation.
load('RMS_Multimeter.mat');


%%%%%%%%%%%%%%%%%%%%%%%%%%%%%%%%%%%%%%%%%%%%%%%%%%%%%%%%%%%%%%%%%%%%%%%
%This figure plots Is, Iload,Iems and Imax ****RMS Values****
figure(1);
```

```
hold on
plot(RMS_Multimeter(1,:),RMS_Multimeter(3,:),'-b','linewidth',2);
plot(RMS_Multimeter(1,:),RMS_Multimeter(4,:),':c','linewidth',2);
plot(RMS_Multimeter(1,:),RMS_Multimeter(5,:),'--m','linewidth',2);
plot(RMS_Multimeter(1,:),RMS_Multimeter(6,:),'--k','linewidth',2);
plot(RMS_Multimeter(1,:),RMS_Multimeter(6,:)/2,':k','linewidth',2);
plot(RMS_Multimeter(1,:),RMS_Multimeter(6,:)-27,'-.k','linewidth',2);
axis([0,max(RMS_Multimeter(1,:)),0,max(RMS_Multimeter(5,:))+1]);
legend('Ils,'Iems','Iload','Imax','Iems On','Imax Off');
xlabel('Time (Seconds)'),ylabel('RMS Current (Amperes)');
title('Source, Load, EMS Current and Current Thresholds');
hold off

%%%%%%%%%%%%%%%%%%%%%%%%%%%%%%%%%%%%%%%%%%%%%%%%%%%%%%%%%%%%%%%%%%%%%%%%%%
%%
%This figure plots Iload_C and Iload_NC, and ***Instantaneous Values***
figure(2);

clear all;
load('Waveforms.mat');
load('Iload_C_waveform.mat');
load('Iload_NC_waveform.mat');

hold on
plot(Waveforms(1,500001:700000),...
    8+Waveforms(2,500001:700000)*1/100,'linewidth',2,'Color',[0.6 0.6
0])
plot(Waveforms(1,500001:700000),...
    6+Iload_C_waveform(2,500001:700000)*1/40,'-b','linewidth',2)
plot(Waveforms(1,500001:700000),...
    4+Iload_NC_waveform(2,500001:700000)*1/40,'-c','linewidth',2)
plot(Waveforms(1,500001:700000),...
    2+Iload_NC_waveform(3,500001:700000)*1/40,'-c','linewidth',2);
plot(Waveforms(1,500001:700000),8.*ones(200000,1),'-k')
plot(Waveforms(1,500001:700000),6.*ones(200000,1),'-k')
plot(Waveforms(1,500001:700000),4.*ones(200000,1),'-k')
plot(Waveforms(1,500001:700000),2.*ones(200000,1),'-k');
axis([Waveforms(1,500001) Waveforms(1,700000) 0 10]);
legend('Vcfil*1/100','Iload C','Iload NC1','Iload NC2');
xlabel('Time (Seconds)');
ylabel('Instantaneous Current (Amperes)/Voltage (Volts)');
title('Critical and Non Critical Load Instantaneous Current over
time');
hold off
```

LIST OF REFERENCES

[1] J. Marqusee. (2012, March 8). Innovation and installation energy. [Online]. Available: http://www.nps.edu/video/portal/Video.aspx?enc=Rp05qxtdJ8MtSo72lcJ4T9895F6NfRNu.

[2] R.H. Lasseter, "MicroGrids" in *Proc. of IEEE Power Engineering Society Winter Meeting,* New York, NY, pp. 305–308, January 2002.

[3] R. H. Lasseter, "Smart distribution: Coupled microgrids," in *Proc. of the IEEE* vol. 99, no. 6, pp. 1074–1082, June 2011.

[4] IEEE Guide for Monitoring, Information Exchange, and Control of Distributed Resources Interconnected with Electric Power Systems, IEEE Standard 1547.3, 2007.

[5] Paolo Piagi and R. H. Lasseter, "Autonomous control of microgrids," in *Proc. of IEEE Power Engineering Society General Meeting*, Montreal, Quebec, June 2006.

[6] M. Godoy Simões, R. Roche, E. Kyriakides, A. Miraoui, B. Blunier, K. McBee1, S. Suryanarayanan, P. Nguyen, and P. Ribeiro, "Smart-Grid technologies and progress in Europe and the USA," in *Proc. of IEEE Energy Conversion Conference and Exposition (ECCE), 2011*, Phoenix, AZ, pp. 383–390, Sep, 2011.

[7] R. Carnieletto, D.I. Brandão, S. Suryanarayanan, F.A. Farret, and M.G. Simões, "Smart grid initiative," *IEEE Industry Applications Magazine*, vol. 17, no. 5, pp. 27–35, Sep/Oct 2011.

[8] D. Boroyevich, I. Cvetković, D. Dong, R. Burgos, F. Wang, and F. Lee, "Future electronic power distribution systems – A contemplative view ," in *Proc. of IEEE 12th International Conference on Optimization of Electrical and Electronic Equipment, OPTIM*, Brasso, Romania, pp. 1369–1380, May 2010.

[9] P.K. Lee and L.L. Lai, "Smart metering in micro-grid applications," in *Proc. of IEEE Power and Energy Society General Meeting*, Calgary, AB, pp. 1–5, July 2009.

[10] R. Majumder, A. Ghosh, G. Ledwich, and F. Zare, "Power management and power flow control with back-to-back converters in a utility connected microgrid," *IEEE Transactions in Power Systems*, vol. 25, no. 2, pp. 821-834, May 2010.

[11] F.Z. Peng, Y.W. Li, and L.M. Tolbert, "Control and protection of power electronics interfaced distributed generation systems in a customer-driven microgrid," in *Proc. of IEEE Power and Energy Society General Meeting*, Calgary, AB, pp. 1-8, July 2009.

[12] F. Blaabjerg, Z. Chen, and S. B. Kjaer, "Power electronics as efficient interface in dispersed power generation systems," *IEEE Trans. on Power Electronics*, vol. 19, pp. 1184–1194, Sept. 2004.

[13] P. Sun, C. Liu, J. Lai, and C. Chen, "Grid-Tie control of cascade dual-buck inverter with wide-range power flow capability for renewable energy applications," *IEEE Trans. on Power Electronics*, vol.27, no.4, April 2012.

[14] Marc Mosko and Victoria Bellotti, "Smart conservation for the lazy consumer" *IEEE Spectrum* vol. 49, pp. 26–30, July 2012.

[15] G. Oriti, A. L. Julian, and N.J. Peck, "Power electronics enabled energy management systems," to be presented at *IEEE Applied Power Electronics Conference (APEC) 2013*, Long Beach, CA, Mar., 2013.

[16] Simulink® by MathWorks [Online] http://www.mathworks.com/products/simulink/

[17] G. Oriti, NPS EC3150 (Power Electronics) Laboratory #5, Naval Postgraduate School, May 2008 (unpublished).

[18] J. E. O'Connor, "Field programmable gate array control of power systems in graduate student laboratories," M.S. thesis, Naval Postgraduate School, Monterey, CA, March 2008.

[19] G. Oriti, D. Zulaica, A.L. Julian, and R. Cristi, "Hardware laboratories for power electronics and motor drives distance learning courses" in *Proc. of IEEE 2nd Energy Conversion Conference and Expo (ECCE) 2010*, Atlanta, GA, Sept 2010.

[20] G. Oriti and A.L. Julian, "Three phase VSI with FPGA based multisampled space vector modulation," *IEEE Trans. on Industry Applications*, vol. 47, no.4, Jul/Aug 2011.

[21] G. Oriti, A.L. Julian, and D. Zulaica, "Doubly fed induction machine drive distance learning laboratory for wind power and electric ship propulsion applications," in *Proc. of IEEE 3rd Energy Conversion Conference and Expo (ECCE)* 2011, Phoenix, AZ, Sep 2011.

[22] Xilinx® "Avnet Virtex-4 LC Development Board," online at: http://www.xilinx.com/products/devkits/DS-KIT-4VLX25LC.htm.

[23] Xilinx “System Generator for DSP -Getting Started Guide” Release 10.1 March, 2008, [Online]. Available: http://www.xilinx.com/support/sw_manuals/sysgen_gs.pdf

[24] XILINX® Products and Services, “ChipScopeTM Pro and the Serial I/O Toolkit,” available online at http://www.xilinx.com/tools/cspro.htm

[25] N. Mohan and T. Undeland, W. P. Robbins, Power Electronics, Converters Applications and Design, third edition, New York: John Wiley and Sons, Inc., 2003.

[26] P. C. Krause, O. Wasynczuk, and S. D. Sudhoff, Analysis of Electric Machinery and Drive Systems, second edition, New York: John Wiley and Sons, Inc., 2002

[27] A. Julian, Single Phase Induction Machine Model, Naval Postgraduate School, Dec. 2011 (unpublished).

[28] G. Oriti, NPS EC3150 (Power Electronics) Laboratory #4, Naval Postgraduate School, May 2008 (unpublished).

THIS PAGE INTENTIONALLY LEFT BLANK

INITIAL DISTRIBUTION LIST

1. Defense Technical Information Center
   Ft. Belvoir, Virginia

2. Dudley Knox Library
   Naval Postgraduate School
   Monterey, California

3. Dr. R. Clark Robertson
   Naval Postgraduate School
   Monterey, California

4. Dr. Giovanna Oriti
   Naval Postgraduate School
   Monterey, California

5. Dr. Alexander L. Julian
   Naval Postgraduate School
   Monterey, California

6. LT Nathan J. Peck
   United States Navy
   Monterey, California